# Strange Attractors from a Parametrical Perspective

Calvin Ashmore
Carnegie Mellon University

# Contents

# 1 Overview

I began this research (unofficially) in the Fall of 2001, when I came across Paul Bourke's page on randomly generated strange attractors [20]. I experimented a great deal with his program to create two dimensional images of attractors based on randomly selected parameters. In a program that I developed, I applied his techniques to three dimensions. This program produced the same sort of objects, but in three dimensional space. My program, however, required many more parameters (a total of ten), which would be randomly generated to produce a vast assortment of orbits, some of which would be the intriguing strange attractors I was after. Eventually I started to wonder about how the images would change when their parameters were varied, and I wrote a small program to make maps of a two dimensional slice of the parameter space. These maps contained some fascinating structures, and some seemingly fractal behavior. This interested me greatly, so I decided to pursue this research formally. I have since written at least a dozen programs to peel away some of the patterns hidden within parameter space, and this paper discusses what I have discovered.

Over the course of this paper, several large areas of dynamics will be addressed. I will discuss quadratic systems and the case of the Hénon map, and then lead into a general discussion of dynamics as a whole. The three particular sets of dynamics are complex dynamics, continuous systems, and discrete systems. Each of these types of systems has some impact on the analysis of strange attractors. Particularly, there are some fascinating analogies that may be made to complex dynamics.

In general, dynamics is a very broad field and its subfields have been thoroughly studied for the most part, however, the analysis of these systems tends to take place mainly in the phase space. The parametrical properties of systems are somewhat harder to investigate, and are less well understood. This paper is aimed towards observing parametrical qualities in a variety of classes of systems; and understanding how certain tools, such as Lyapunov exponents, translate between these different systems.

## 1.1 Goals

In my initial investigation of the parameter space around randomly chosen strange attractors, I saw a variety of peculiar fractal properties in the parameter space maps. In the regions which diverge to infinity, there are features that would have self similar structure. It was conceivable that the entire space, not just any cross section, had self similar structure and was fractal. However, some other problems became evident. What initial point should be used, and what changes as that is varied? Why are some cross sections smooth and others jagged? What do the maps say about the more detailed behavior of the orbits in those regions of parameter space? Are there regions of the map which only produce orbits with one cycles, or two cycles, and so on? The purpose of this research was to explore and begin to understand these dynamics, investigating and potentially answering as many of these questions as possible.

The color images on the following page are some of the original parameter maps that I had made. Note the strange self similar structure in the last one. This appeared to be indicative of a fractal structure originally, but after this current research, the black regions were likely areas where the chosen initial point

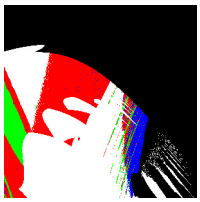

Figure 1:

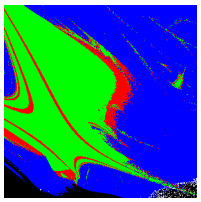

Figure 2:

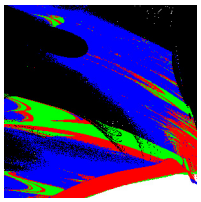

Figure 3:

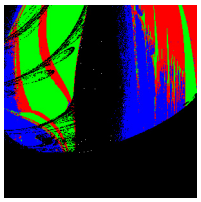

Figure 4:

did not fall within the basin of attraction for the attractor. The importance of the choice of initial point will be described in detail later.

## 1.2 Dynamical Systems

Dynamics involves the study of a point in a metric space which is being moved about by either a function in discrete steps, or by a differential equation governing its trajectory. Most of this paper shall be concerned with discrete systems, but continuous systems will be discussed in Section 5. Suppose our system is discrete, and we are observing the iterates of a point $x$. Depending on the initial point and the function, one of the following will occur:

1. The point stays fixed
2. The point is in an $n$-cycle, and the $n^{th}$ iterate of $x$ is $x$ itself.
3. The point approaches a fixed point
4. The point approaches a cycle
5. The orbit of the point is unbounded
6. The point does none of the above; it remains bounded and neither cycles nor approaches a cycle

In the last example, the behavior is typically described as chaotic, and this is the case where it is possible to find strange attractors.

In this paper we shall examine relatively simple systems with a low dimension, from a geometrical perspective. In cases where the system is complicated or its dimension is high, it is more appropriate to use statistical analysis to extract useful information from the orbits of points. This kind of study is called egrodic theory, which makes use of invariant probability measure over the phase space. This paper focuses on geometrical analysis of systems, specifically regarding fixed points and cycles, and the overall fractal structure of certain regions in both parameter and phase space. As such, ergodic theory and the issues it raises do not bear much of a part in this paper, but is worth mentioning for reference.

Typically when one investigates a dynamical system, it is in order to predict the system's long term behavior. Geometric analysis focuses on the properties of attracting points and cycles, and observes what points fall into what cycles. The behavior of fixed points and cycles tends to govern the entire dynamics of the system, and by understanding what the fixed points do, it is usually possible to make some inferences about the orbits of points under the system.

## 2 Preliminaries and Notation

There are a few terms and basic habits of notation that shall be used throughout this paper. Let $\mathsf{X} = \mathbb{R}^N$ be the **phase space** or point space. Typically we are concerned with a function $f \in \mathsf{X} \to \mathsf{X}$ that maps $\mathsf{X}$ onto itself. Usually $f$ is parameterized by some $\boldsymbol{a} \in \mathsf{P}$ in the parameter space, $\mathsf{P} \subset \mathbb{R}^M$. When the distinction between different parameters is important, we shall use the term $f_{\boldsymbol{a}}$. Both $\mathsf{X}$ and $\mathsf{P}$, by being subsets of Euclidean space, are metric spaces, and occasionally we will use some norm $\|\cdot\|$ for analytic purposes on one of those spaces. Usually the exact norm is not important, but will be referred to specifically, when it is relevant.

In subsequent sections I shall repeatedly refer to matrix and vector norms, but the results within do not usually depend on which base norm is used. The matrix norm is always derived from the vector norm as follows:

$$\|A\| = \max_{\|\boldsymbol{x}\|=1} \|A\boldsymbol{x}\|$$

We are concerned with the long term behavior of points in the phase space under iterations of $f$. Consider $\boldsymbol{x}_0$ as an initial point, the $n$-th iterate of $f$ on $\boldsymbol{x}_0$ is defined as $f^n(\boldsymbol{x}_0)$. Depending on the function and the initial point, the point may do one of several things.

An orbit may be **unbounded**, in which case, $\forall s \in \mathbb{R}$, $\exists n \in \mathbb{N}$, such that $\|f^n(\boldsymbol{x}_0)\| > s$. Specifically, if the orbit is unbounded, and if $\forall s \in \mathbb{R}$, $\exists N \in \mathbb{N}$ such that $\forall n > N$, $\|f^n(\boldsymbol{x}_0)\| > s$, then the point is said to **diverge to infinity**. If $f(\boldsymbol{x}_0) = \boldsymbol{x}_0$, then $\boldsymbol{x}_0$ is **fixed**. If $f^p(\boldsymbol{x}_0) = \boldsymbol{x}_0$, where $p$ is the least such number such that this holds, then $\boldsymbol{x}_0$ is **periodic with period** $p$. Fixed points are naturally periodic with period 1. Unless chosen carefully, a point will not start out fixed or cyclic, but may tend towards a fixed point or a cycle. A point $\boldsymbol{x}_0$ **tends to a cycle with period** $p$ if $\exists \boldsymbol{y} \in \mathsf{X}$ which is cyclic with period $p$, and $\forall \epsilon > 0$, $\exists N \in \mathbb{N}$ such that $\forall n > N$, $\|f^n(\boldsymbol{x}_0) - f^n(\boldsymbol{y})\| < \epsilon$. If none of these occur, then $\boldsymbol{x}_0$ is both bounded under $f$ and it does not fall into any sort of cyclic behavior. In this situation the point is almost certainly chaotic.

It is fairly important to clearly define the term chaos. The term is frequently used, and often misused, but it does describe a clear mathematical property of dynamical systems. We say a system is **chaotic** at a point $\boldsymbol{x}_0$ if iterates of points arbitrarily close to $\boldsymbol{x}_0$ become distant from the corresponding iterates of $\boldsymbol{x}_0$ under applications of $f$. More precisely: $\exists \delta > 0$ such that $\forall \epsilon > 0$, $\forall \boldsymbol{y} \in B_\epsilon(\boldsymbol{x}_0) \backslash \{\boldsymbol{x}_0\}$ implies that $\exists N \in \mathbb{N}$ such that $d(f^N(\boldsymbol{y}), f^N(\boldsymbol{x}_0)) \geq \delta$. For our purposes, these iterates must remain bounded: $f = \boldsymbol{x} \mapsto 2\boldsymbol{x}$ is may not be defined as chaotic, even though distance between points doubles under $f$. In the scope of this paper, an unbounded orbit will not considered to be chaotic, even though there may be bijective transformations that may convert the orbit between bounded and unbounded coordinate systems.

Fixed points may attract or repel nearby points. It will be demonstrated via Lemma 1 that if $\boldsymbol{x}_0$ is fixed, and the norm of the derivative, $\|f'(\boldsymbol{x}_0)\|$, is less than one, then that particular point draws in its neighbors. In this case, $\exists \epsilon > 0$, $\exists C < 1$ such that $\|f(\boldsymbol{x}) - f(\boldsymbol{x}_0)\| = \|f(\boldsymbol{x}) - \boldsymbol{x}_0\| \leq C\|\boldsymbol{x} - \boldsymbol{x}_0\|$. When this occurs the point is said to be **strongly attracting**. With a strongly attracting fixed point, the function contracts balls around $\boldsymbol{x}_0$. The term "strong" is really quite appropriate: it will be seen later that some fixed points may draw in nearby

points, but not have this extra condition, those are called **weakly attracting** fixed points. With a weakly attracting fixed point, there is an open ball around $\boldsymbol{x}_0$ such that every point in the ball tends towards $\boldsymbol{x}_0$. That is, $\exists \epsilon > 0$ such that $\forall \boldsymbol{y} \in B_\epsilon(\boldsymbol{x}_0)$, $\boldsymbol{y}$ tends to $\boldsymbol{x}_0$ under $f$. Weakly attracting fixed points also behave similar (though not exactly) to neutral fixed points in complex analysis.

Another pair of useful terms to describe long term behavior are the **Ω-limit set** and the **A-limit set**. The Ω-limit set of $\boldsymbol{x}_0$ is the set of cluster points of the point's forward orbit. That is:

$$\Omega_{lim}(\boldsymbol{x}_0) = \bigcap_{n \in \mathbb{N}} \overline{\{f^k(\boldsymbol{x}_0) \,|\, \forall k > n\}}$$

This definition allows us to make a few very helpful points. The period of an orbit starting from $\boldsymbol{x}_0$ can be neatly represented as $period(\boldsymbol{x}_0) = \#\Omega_{lim}(\boldsymbol{x}_0)$. Depending on the long term behavior of $\boldsymbol{x}_0$ under $f$, the period changes accordingly. If $\boldsymbol{x}$ escapes to $\infty$, $\Omega_{lim}(\boldsymbol{x}_0)$ will of course be empty. If $\boldsymbol{x}$ falls into a fixed point or cycle, then the limit set will consist of the fixed point or each point in the cycle. If $\boldsymbol{x}_0$ becomes chaotic, then $\Omega_{lim}(\boldsymbol{x}_0)$ will be an infinite set, probably having some nonintegral fractal dimension.

The A-limit set, pronounced "capital-alpha", of a point $\boldsymbol{x}_0$ is conversely the set of the limit points of all of the backwards iterates of $\boldsymbol{x}_0$ under $f$. Typically, points have multiple preimages, so we may think of $f^{-k}(\boldsymbol{x}_0)$ as $\{\boldsymbol{x} \in \mathsf{X} \,|\, f^k(\boldsymbol{x}) = \boldsymbol{x}_0\}$. Thus it's possible to define the A-limit set as:

$$\mathrm{A}_{lim}(\boldsymbol{x}_0) = \bigcap_{n \in \mathbb{N}} \overline{\bigcup_{k > n} f^{-k}(\boldsymbol{x}_0)}$$

One of the most important terms we will use is the **basin of attraction**. This is defined, for a set of points $S$, as $\mathrm{A}(S) = \{\boldsymbol{x} \in \mathsf{X} \,|\, \Omega_{lim}(\boldsymbol{x}) = S\}$. In other words, the basin of attraction for a set is the collection of points which eventually becomes drawn to that set. If $S$ is not the Ω-limit set of any other set, the basin of attraction of $S$ will be empty. If a cycle is repelling, its basin of attraction is just the cycle itself. Strange attractors have basins of attraction as well, and these are often irregularly shaped. One particular term which deserves special attention is the **basin of attraction of infinty**, this describes all points which eventually wind up diverging to infinity,

$$\mathrm{A}(\infty) = \{\boldsymbol{x} \in \mathsf{X} \,|\, \forall \epsilon > 0,\, \exists N \in \mathbb{N},\, \forall n > N,\, \|f^n(\boldsymbol{x})\| > \epsilon\}.$$

In Complex Analysis, the compliment of this, $\mathsf{X} - \mathrm{A}(\infty)$, is called the filled-in Julia set. I'll refer to this as the filled-in Julia-**like** set for the nonconformal case to avoid abusing the term "Julia set".

One term that will be used very frequently is the **Lyapunov exponent**. This is a term that is applied to both the discrete and continuous case, and represents predictability of the system. For an $N$ dimensional system, the Lyapunov exponent is a vector with dimension $N$. Like the eigenvalues of a matrix, it is often useful to arrange the Lyapunov exponent in order of descending value, $\nu_1 \geq \nu_2 \geq \cdots \geq \nu_N$. The exponent will always be sorted in this way in this paper. When $\nu_1$ is positive, then nearby points in phase space tend to separate under the mapping $f$. Since chaos is when nearby points will separate over time in a bounded system, chaos is synonymous with that system having a positive

Lyapunov exponent. If $\nu_1$ is negative, then points will typically converge to an attracting cycle of some kind. $\nu_1$ is the most important part of the exponent, and when we refer to the Lyapunov exponent of an orbit as just a single number, this is always $\nu_1$. The spectrum of Lyapunov exponents has the potential to describe in detail the dynamics of a system, but this will be elaborated upon later.

# 3 Quadratic Systems

At the moment, we do not need to consider the entire breadth of discrete dynamical systems, so here we will focus on systems of the form:

$$f(\boldsymbol{x})_i = \sum_{j=1}^{N}\sum_{k=1}^{N} a_{ijk}\boldsymbol{x}_j\boldsymbol{x}_k + \sum_{j=1}^{N} b_{ij}\boldsymbol{x}_j + c_i$$

Quadratic systems are also nice to study because they tend to just fold the phase space. Thus we can understand the behavior of the system by examining the way the function folds the phase space. Certain areas of the phase space can appear to be kneaded under iterations of the map. This is what occurs with the logistic map $x \mapsto 4x(1-x)$. Points evenly spaced on the unit interval will become mixed under the logistic map, as though they were kneaded together. This phenomenon often occurs with quadratic functions in arbitrary dimensions.

## 3.1 Result regarding strongly attracting fixed points

**Lemma 1** *The matrix norm of the derivative of a differentiable function at a fixed point is less than one if and only if the fixed point is strongly attracting.*

This lemma is true regardless of the norm used (and is true for any type of differentiable function). The claim is that strong attraction at a fixed point $\boldsymbol{x}_0$ implies that $\|f'(\boldsymbol{x}_0) < 1\|$.

First suppose $f$ is strongly attracting at $\boldsymbol{x}_0$. Let $\epsilon > 0$ and $C < 1$ such that $\|f(\boldsymbol{x}) - f(\boldsymbol{x}_0)\| \leq C\|\boldsymbol{x} - \boldsymbol{x}_0\|$ for all $\boldsymbol{x}$ such that $\|\boldsymbol{x} - \boldsymbol{x}_0\| < \epsilon$. For any $\mu > 0$, $\exists\delta \in (0, \epsilon)$ such that:

$$\|f(\boldsymbol{x}) - f(\boldsymbol{x}_0) - f'(\boldsymbol{x}_0)(\boldsymbol{x} - \boldsymbol{x}_0)\| \leq \mu\|\boldsymbol{x} - \boldsymbol{x}_0\|$$

for all $\boldsymbol{x}$ such that $\|\boldsymbol{x} - \boldsymbol{x}_0\| \leq \delta$. Thus:

$$\begin{aligned}
\|f'(\boldsymbol{x}_0)\| &= \sup_{0<\|\boldsymbol{x}-\boldsymbol{x}_0\|\leq\delta} \frac{\|f'(\boldsymbol{x}_0)(\boldsymbol{x} - \boldsymbol{x}_0)\|}{\|\boldsymbol{x} - \boldsymbol{x}_0\|} \\
&= \sup_{0<\|\boldsymbol{x}-\boldsymbol{x}_0\|\leq\delta} \frac{\|f(\boldsymbol{x}) - f(\boldsymbol{x}_0)\| - [\|f(\boldsymbol{x}) - f(\boldsymbol{x}_0) - f'(\boldsymbol{x}_0)(\boldsymbol{x} - \boldsymbol{x}_0)\|]}{\|\boldsymbol{x} - \boldsymbol{x}_0\|} \\
&\leq \sup_{0<\|\boldsymbol{x}-\boldsymbol{x}_0\|\leq\delta} \left[\frac{\|f(\boldsymbol{x}) - f(\boldsymbol{x}_0)\|}{\|\boldsymbol{x} - \boldsymbol{x}_0\|} + \frac{\|f(\boldsymbol{x}) - f(\boldsymbol{x}_0) - f'(\boldsymbol{x}_0)(\boldsymbol{x} - \boldsymbol{x}_0)\|}{\|\boldsymbol{x} - \boldsymbol{x}_0\|}\right] \\
&\leq \sup_{0<\|\boldsymbol{x}-\boldsymbol{x}_0\|\leq\delta} (C + \mu) \\
&= C + \mu
\end{aligned}$$

And we can choose $\mu$ such that $C + \mu < 1$ and establish that $\|f'(\boldsymbol{x}_0)\| < 1$.

Next we show the converse, and assume $\|f'(\boldsymbol{x}_0)\| < 1$. Let $\mu > 0$. Again, there must exist $\epsilon > 0$ such that:

$$\|f(\boldsymbol{x}) - f(\boldsymbol{x}_0) - f'(\boldsymbol{x}_0)(\boldsymbol{x} - \boldsymbol{x}_0)\| \leq \mu\|\boldsymbol{x} - \boldsymbol{x}_0\|$$

for all $\boldsymbol{x}$ such that $\|\boldsymbol{x} - \boldsymbol{x}_0\| < \epsilon$. Thus:

$$\begin{aligned}
\|f(\boldsymbol{x}) - f(\boldsymbol{x}_0)\| &= \|f(\boldsymbol{x}) - f(\boldsymbol{x}_0) - f'(\boldsymbol{x}_0)(\boldsymbol{x} - \boldsymbol{x}_0) + f'(\boldsymbol{x}_0)(\boldsymbol{x} - \boldsymbol{x}_0)\| \\
&\leq \|f(\boldsymbol{x}) - f(\boldsymbol{x}_0) - f'(\boldsymbol{x}_0)(\boldsymbol{x} - \boldsymbol{x}_0)\| + \|f'(\boldsymbol{x}_0)(\boldsymbol{x} - \boldsymbol{x}_0)\| \\
&\leq \mu\|\boldsymbol{x} - \boldsymbol{x}_0\| + \|f'(\boldsymbol{x}_0)\|\|\boldsymbol{x} - \boldsymbol{x}_0\| \\
&= (\mu + \|f'(\boldsymbol{x}_0)\|)\|\boldsymbol{x} - \boldsymbol{x}_0\|
\end{aligned}$$

It is possible choose a value of $\mu$ such that $\mu + \|f'(\boldsymbol{x}_0)\| < 1$, and we find that $f$ is strongly attracting at $\boldsymbol{x}_0$.

Note that this part of the proof does not specifically require that $\boldsymbol{x}_0$ be a fixed point. The map will contract at this point regardless, pulling in neighbors to the image of $\boldsymbol{x}_0$ under $f$.

**Theorem 1** *Quadratic systems have at most one strongly attracting fixed point.*

This may come as a surprise since there are functions of this form which have multiple fixed points, the eigenvalues of whose derivatives are less than one. Recall that if $\boldsymbol{p}$ is a strongly attracting fixed point under $f$, then $\|f'(\boldsymbol{p})\| < 1$. Thus what remains to be shown is that there is at most one fixed point such that the norm of its derivative is less than one. If $f$ is a polynomial of degree 2, then its derivative will be an affine linear operator. So we note that $\boldsymbol{x} \mapsto f'(\boldsymbol{x})$ is an affine linear operator, and the set of points $B \subset \mathsf{X}$, where $B = \{\boldsymbol{x} \in \mathsf{X} \,|\, \|f'(\boldsymbol{x})\| < 1\}$ is a convex set. The proof is as follows:

Let $B = \{\boldsymbol{x} \in \mathsf{X} \,|\, \|f'(\boldsymbol{x})\| < 1\}$.

$$\forall \boldsymbol{x} \in \mathsf{X},\ \exists M_{\boldsymbol{x}} \in \mathsf{X} \times \mathsf{X},\ \boldsymbol{b} \in \mathsf{X},\ \text{such that: } f'(\boldsymbol{x})\boldsymbol{y} = M_{\boldsymbol{x}}\boldsymbol{y} + \boldsymbol{b}$$

Also; $M_{\boldsymbol{x}}$ is linear in $\boldsymbol{x}$, since $f$ is quadratic. Let $\boldsymbol{s}, \boldsymbol{t} \in B$ and set $\boldsymbol{u} = (1 - \alpha)\boldsymbol{s} + \alpha\boldsymbol{t}$. Thus if $\|\boldsymbol{y}\| = 1$,

$$\begin{aligned}
\|f'(\boldsymbol{u})\boldsymbol{y}\| &= \|M_{\boldsymbol{u}}\boldsymbol{y} + \boldsymbol{b}\| = \|M_{[(1-\alpha)\boldsymbol{s}+\alpha\boldsymbol{t}]}\boldsymbol{y} + \boldsymbol{b}\| \\
&= \|(M_{(1-\alpha)\boldsymbol{s}} + M_{\alpha\boldsymbol{t}})\boldsymbol{y} + \boldsymbol{b}\| \\
&= \|(1 - \alpha)(M_{\boldsymbol{s}}\boldsymbol{y} + \boldsymbol{b}) + \alpha(M_{\boldsymbol{t}}\boldsymbol{y} + \boldsymbol{b})\| \\
&\leq (1 - \alpha)\|f'(\boldsymbol{s})\boldsymbol{y}\| + \alpha\|f'(\boldsymbol{t})\boldsymbol{y}\| \leq (1 - \alpha)\|f'(\boldsymbol{s})\| + \alpha\|f'(\boldsymbol{t})\| \\
&< (1 - \alpha) \cdot 1 + \alpha \cdot 1 = 1
\end{aligned}$$

Thus we can see that $\|f'(\boldsymbol{u})\boldsymbol{y}\| < 1$, so $\boldsymbol{u} \in B$.

Suppose now there are two strongly attracting fixed points, $\boldsymbol{p}$ and $\boldsymbol{q}$. Thus $\|f'(\boldsymbol{p})\| < 1$ and $\|f'(\boldsymbol{q})\| < 1$, and so both $\boldsymbol{p}$ and $\boldsymbol{q}$ are in $B$. Because $B$ is convex, the segment $\overline{\boldsymbol{pq}} \subset B$. Because of Lemma 1, we know that for each $\boldsymbol{x} \in \overline{\boldsymbol{pq}}$, there exists $\delta_{\boldsymbol{x}} > 0$, $C_{\boldsymbol{x}} < 1$ such that $\|f(\boldsymbol{y}) - f(\boldsymbol{x})\| \leq C_x\|\boldsymbol{y} - \boldsymbol{x}\|$ for all $\boldsymbol{y}$ such that $\|\boldsymbol{y} - \boldsymbol{x}\| < \delta_{\boldsymbol{x}}$. Because $\{B_{\delta_{\boldsymbol{x}}}(\boldsymbol{x}) \,|\, \boldsymbol{x} \in \overline{\boldsymbol{pq}}\}$ is an open cover of the compact set $\overline{\boldsymbol{pq}}$, we can find a finite sub-cover.

Let $\boldsymbol{x}(\alpha) = (1-\alpha)\boldsymbol{p} + \alpha\boldsymbol{q}$. Then we obtain $0 = \alpha_0 < \alpha_a < \cdots < \alpha_N = 1$, $\boldsymbol{x}_j = \boldsymbol{x}(\alpha_j)$ and balls $B_j$, $0 \leq j \leq N$, $B_j = B_{\delta_{\boldsymbol{x}_j}}(\boldsymbol{x}_j)$, with $B_j \cap B_{j+1} \neq \emptyset$ for all $0 \leq j < N$, which defines our finite open cover. Now select $\boldsymbol{z}_j \in B_j \cap B_{j+1} \cap \overline{\boldsymbol{pq}}$ for $0 \leq j < N$ with $\|\boldsymbol{x}_j - \boldsymbol{z}_j\| + \|\boldsymbol{z}_j - \boldsymbol{x}_{j+1}\| = \|\boldsymbol{x}_j - \boldsymbol{x}_{j+1}\|$. Then:

$$\begin{aligned}
\|f(\boldsymbol{p}) - f(\boldsymbol{q})\| &\leq \|f(\boldsymbol{x}_0) - f(\boldsymbol{z}_0)\| + \|f(\boldsymbol{z}_0) - f(\boldsymbol{x}_1)\| + \|f(\boldsymbol{x}_1) - f(\boldsymbol{z}_1)\| + \\
&\quad \|f(\boldsymbol{z}_1) - f(\boldsymbol{x}_2)\| + \|f(\boldsymbol{x}_2) - f(\boldsymbol{z}_2)\| + \|f(\boldsymbol{z}_2) - f(\boldsymbol{x}_3)\| + \\
&\quad \cdots + \|f(\boldsymbol{x}_{N-1} - f(\boldsymbol{z}_{N-1})\| + \|f(\boldsymbol{z}_{N-1}) - f(\boldsymbol{x}_N)\| \\
&\leq C_{\boldsymbol{x}_0}\|\boldsymbol{x}_0 - \boldsymbol{z}_0\| + C_{\boldsymbol{x}_1}\|\boldsymbol{z}_0 - \boldsymbol{x}_1\| + C_{\boldsymbol{x}_1}\|\boldsymbol{x}_1 - \boldsymbol{z}_1\| + \\
&\quad C_{\boldsymbol{x}_2}\|\boldsymbol{z}_1 - \boldsymbol{x}_2\| + C_{\boldsymbol{x}_2}\|\boldsymbol{x}_2 - \boldsymbol{z}_2\| + C_{\boldsymbol{x}_3}\|\boldsymbol{z}_2 - \boldsymbol{x}_3\| + \\
&\quad \cdots + C_{\boldsymbol{x}_{N-1}}\|\boldsymbol{x}_{N-1} - \boldsymbol{z}_{N-1}\| + C_{\boldsymbol{x}_N}\|\boldsymbol{z}_{N-1} - \boldsymbol{x}_N\| \\
&\leq [\max_{0\leq j\leq N} C_{\boldsymbol{x}_j}](\|\boldsymbol{x}_0 - \boldsymbol{z}_0\| + \|\boldsymbol{z}_0 - \boldsymbol{x}_1\| + \|\boldsymbol{x}_1 - \boldsymbol{z}_1\| + \\
&\quad \|\boldsymbol{z}_1 - \boldsymbol{x}_2\| + \cdots + \|\boldsymbol{x}_{N-1} - \boldsymbol{z}_{N-1}\| + \|\boldsymbol{z}_{N-1} - \boldsymbol{x}_N\|) \\
&\leq [\max_{0\leq j\leq N} C_{\boldsymbol{x}_j}]\|\boldsymbol{p} - \boldsymbol{q}\| \\
&< \|\boldsymbol{p} - \boldsymbol{q}\|, \text{ only if } \boldsymbol{p} \neq \boldsymbol{q}.
\end{aligned}$$

Therefore, $d(f(\boldsymbol{p}), f(\boldsymbol{q})) < d(\boldsymbol{p}, \boldsymbol{q})$, but since $\boldsymbol{p}$ and $\boldsymbol{q}$ are fixed points, they must be the same attracting fixed point. This completes the proof.

## 3.2 Conjecture regarding attracting cycles

**Conjecture 1** *Quadratic systems may have at most one strongly attracting cycle.*

Given Theorem 1, it also seems reasonable to suppose that there may be only one strongly attracting cycle, but this is much harder to show. A strongly attracting cycle of period $p$ is an ordinary cycle for which the derivative of $f^p$ is less than one at the points in the cycle. There may, however, be multiple weakly attracting fixed points, as evidenced on page 15. Over the course of my investigation, I was unable to derive a proof either for or against this claim, even in spite of some suggestive numerical evidence, which shall be presented in the next section. The crux of the problem is that because the function is iterated, the $n^{\text{th}}$ derivative ceases to be affine. For an $n$-cycle to be strongly attracting, each $f^n$ must have each $\boldsymbol{x}_j$ as an attracting fixed point, in other words, the following must hold:

$$\forall j \in 1..n,\ \|(f^n)'(\boldsymbol{x}_j)\| < 1$$

It would be enough to show there can not be more than two strongly attracting cycles of the same period $n$, by taking the lowest common multiple. Due to the laws of matrix multiplication, it is not possible to claim that $\prod_{j=1}^{n} \|f'(\boldsymbol{x}_j)\| < 1$, in which case there would be one point the norm of whose derivative is less than one, which would be instrumental in building a proof. This problem becomes difficult because of the loss of commutativity in matrix multiplication. However, it also means that if a proof could be established, it would be a very strong result.

In one dimension this is not a concern, and the conjecture does hold. By results in complex analysis [2], we know that in $\hat{\mathbb{C}}$ ($\mathbb{C}$ extended to include $\infty$), there are at most two attracting cycles for a rational function of degree 2. This includes the point $\infty$, which is also attracting under any polynomial of degree $d \geq 2$. Since $\mathbb{R} \subset \hat{\mathbb{C}}$, we have that there can only be one attracting cycle that is not infinite, therefore our conjecture holds for one dimension. Matrix multiplication makes things egregiously complicated, and I have thus been unable to find a result one way or another.

### 3.3 Results of numerical experiments

I developed a program to test for strongly attracting cycles using random points in parameter space, specifically in the two dimensional case, which is starting point to analyze $n$-dimensional space. The program tests for some stable cycle and determines whether the cycle is strongly attracting. If so, the program proceeds to attempt to locate other attracting cycles. The program also discards orbits that are measured to have a positive Lyapunov exponent. In an earlier investigation, I did not reject these, and had on my hands a number of false positives (only about 1 in 100000 tests) which appeared to have multiple strongly attracting cycles, but in reality they were orbits that would converge to one cycle very slowly. Alternately there might be a weakly attracting cycle that simply appeared to be strongly attracting due to numerical error, or an orbit may have a lyapunov exponent that measures positive (implying instability), but the orbit seems to the program to be converging to a cycle. It remains to be proven formally whether it is possible for an attracting cycle and a chaotic orbit can coexist in a quadratic function.

One possible reason for the false positives is that the parameters were chosen in between two configurations with different attracting cycles, and this forms a chaotic region in parameter space between them. Generally these systems will wind up always falling into one orbit or into chaos.

Overall, the program was not able to find simultaneous strongly attracting cycles. Though, due to the somewhat buggy nature of the program and results, this cannot be counted as conclusive evidence of the conjecture. It does seem unlikely that there would be two strongly attracting cycles unless chaos were present. On the other hand, if there were chaos present, it would seem unlikely that there could be two cycles that are attracting. There were situations in which there sometimes seemed to be strongly attracting cycles (usually fixed points) and also chaos. This is a situation that definitely warrants further investigation, specifically of the following questions. If chaos is present in a quadratic system, can cycles actually be attracting? What are the properties of any systems which have multiple (at least) weakly attracting cycles, and chaos is present?

Despite these concerns, the results of the program support the claim that there may only be one strongly attracting cycle. The following is output from the program after being run on one million points randomly chosen in parameter space.

| | |
|---|---|
| Total Tests: | 1000000 |
| Stable Structures: | 47937 |
| Chaotic structures: | 33279 |
| Nonattracting periodic: | 12890 |
| Valid periodic: | 1768 |
| Two Structures: | 29 |
| Period and Chaos: | 13 |
| Period and Period: | 16 |

The program chooses points in the parameter space for the mapping:

$$x_{n+1} = a_1 x_n^2 + a_2 x_n y_n + a_3 y_n^2 + a_4 x_n + a_5 y_n + a_6$$

$$y_{n+1} = b_1 x_n^2 + b_2 x_n y_n + b_3 y_n^2 + b_4 x_n + b_5 y_n + b_6$$

Each value $a_j$ and $b_k$ is chosen randomly between $-2$ and 2. Then 100 random initial points $(x, y)$ are chosen in $[-2, 2]\times[-2, 2]$. If there is a pair which does not escape to infinity, and its orbit is not chaotic, then it must be in a cycle. If that cycle is strongly attracting, the program attempts to locate another strongly attracting cycle which differs than the original one. It tests for these 20 times, each time it chooses 100 random initial points to find one that does not go to infinity, is not chaotic, and is separate from the original cycle.

The source code for the program which generated this data can be found in Appendix A.2.

## 3.4 Parameter Space

Much of the research that has been done on strange attractors and dynamics in general has had a fairly heavy-handed focus on dynamics from the point of view of the phase space. Examining parameter space can yield general information on what sorts of dynamics can possibly arise for any point chosen in a system under a specific set of parameters.

## 3.5 Specific case of the Hénon attractor

The Hénon map is a very simple system in two dimensions with two parameters. It nontheless holds a very rich parameter space, containing many interesting varieties of dynamical phenomena. The formula I shall use for the Hénon map is as follows:

$$\begin{aligned} x_{n+1} &= a - x_n^2 + b y_n \\ y_{n+1} &= x_n \end{aligned}$$

It is classically regarded as one of the simplest strange attractors. This is largely because it has a constant Jacobian: $-b$. The Jacobian is calculated as the determinant of the derivative of the map. Since it is fixed, we know that the map is always invertible for $b \neq 0$. The Hénon attractor is frequently recognized as having a kneaded parabolic shape (for $a = 1.4$ and $b = .3$), though that is only for one possible configuration of parameters. There is a wide range of possible behavior that the map can exhibit, which includes cycles of all periods, as well as a large variety of chaotic behaviors.

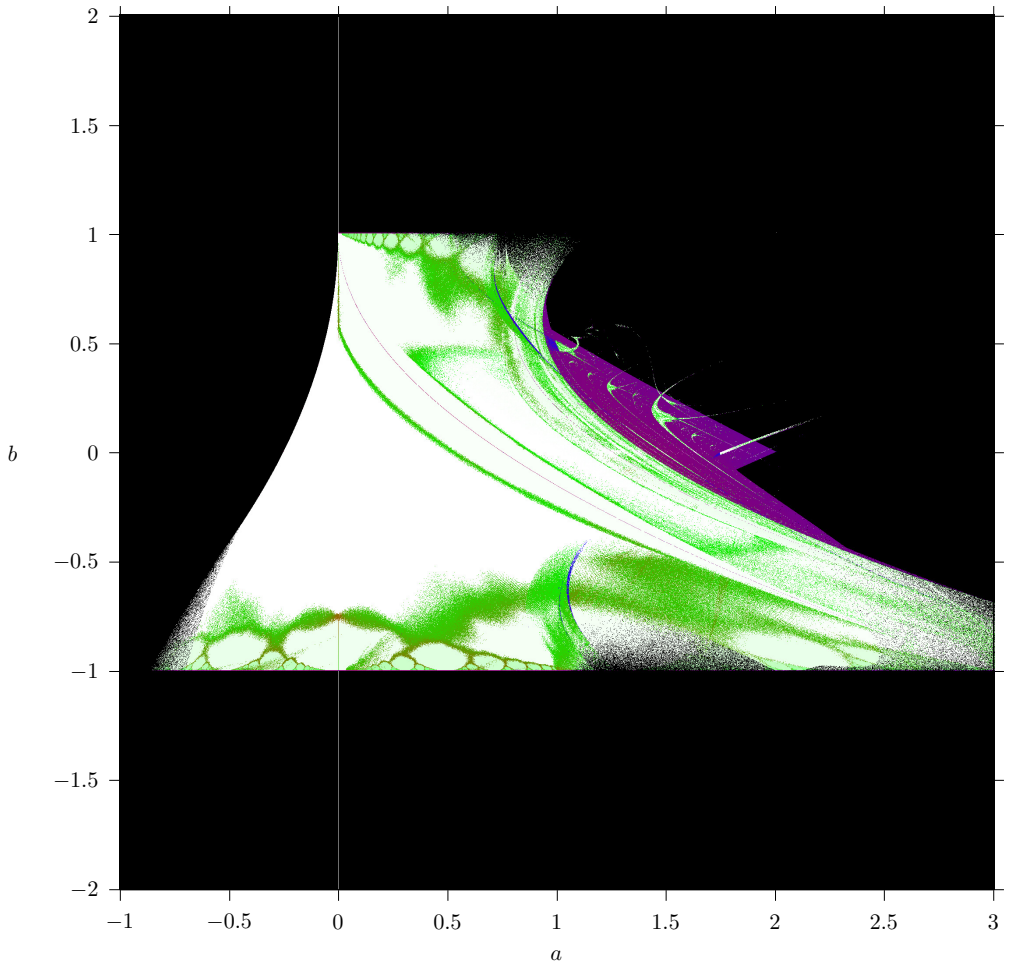


Figure 5: The full Henon parameter map.

### 3.6 Parameter maps and what different areas mean

Comprehensively describing parameter space is inherently very tricky. Information represented in parameter space must allow an observer to make claims about structure and behavior in the phase space. However, it is not easy to test for all the different types of structures in the phase space. Randomly chosen points may fall into the orbits of different attractors, or sometimes there may be a stable orbit which is hard to observe, because its basin of attraction is very small and everything around it diverges to infinity. For the quadratic polynomial in the complex plane, $z \mapsto z^2 + c$, the system dynamics hinge on the forward iterates of 0, which is a critical point. This is not the case for the Hénon map and for other systems. I have attempted to resolve this problem by sampling several randomly chosen points in the phase space for each point in parameter space.

Here is the Hénon parameter map in all its complexity. What each portion of it means and represents shall be explained shortly:

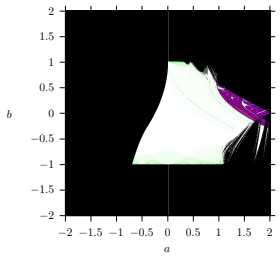


Figure 6: The parameter map using initial point $(0, 0)$.

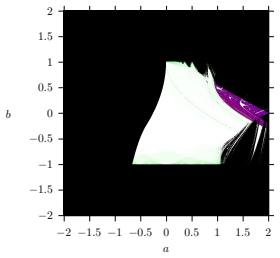


Figure 7: The parameter map using initial point $(-0.1, 0)$.

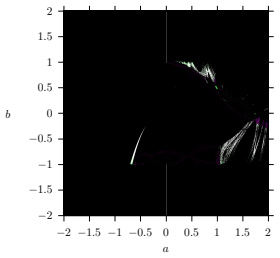


Figure 8: The difference between the two.

Around the region nearby $(a, b) = (1.5, -0.5)$ in the parameter space, the attracting structures were so far away from the origin that my initial programs would reveal this area as a strange self-similar structure in which every point inside would go to infinity. In plotting the Julia-like sets it became apparent that this was not the case, but rather the bulk of the filled-in Julia-like set was far away from the origin. To illustrate the difference this makes, below are two images of the parameter map with only one chosen initial point, and beside those are the differences in the images (Figures 6-8). The light colored regions are the areas where the two are different. The self similar structures vary considerably with the change in the initial point, and don't seem to be tremendously indicative of any real dynamics taking place there. A good analogy to this is plotting the Mandelbrot set by only examining the forward orbits of the point $0.1 + 0.1i$, instead of 0. Some sections of the Mandelbrot set would simply disappear! When a larger sample space is considered, (my program tests random points near both $(0, 0)$ and $(0, -1)$) the parameter space appears to be much cleaner.

In order to express the most information about the two dimensional parameter space via these images, color is used to represent a variety of things. Black suggests that the area is unstable and goes to infinity. Specifically, it means a random sampling of points all escaped to infinity. Earlier in my investigation, it became clear that the seemingly unstable areas discussed above were the result of the Julia-like set moving away from the origin, gray colors were used in the parameter maps to indicate that some randomly chosen initial points would stay bounded while others would not. Now I do not use the gray colors, but instead display the color normally if there is at least one bounded orbit.

White and light green colors indicate that there are periodic orbits with negative Lyapunov exponents. In these areas, sampled points would fall into some kind of strongly attracting cycle. A purer green indicates a longer cycle. It is difficult to tell the difference between areas where the difference between the length of the cycles is small, so there are some images below to help clarify where areas have only one cycle with periods one through eight.

Dark green and red indicate that there exist multiple at-least weakly attracting cycles. This green is much darker than in the cyclic regions described above, so there won't be any mistaking one for the other. These are colored according to the Lyapunov exponent. When the area is more red, the exponent is more positive, and points chosen in that area behave in a more chaotic fashion.

Figure 9: Period 1

Figure 10: Period 2

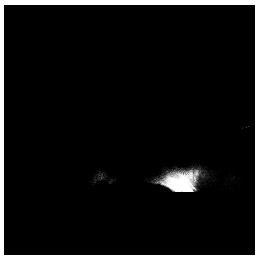

Figure 11: Period 3

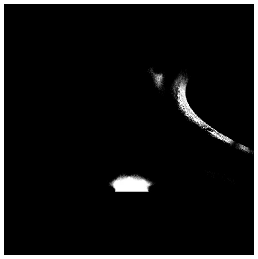

Figure 12: Period 4

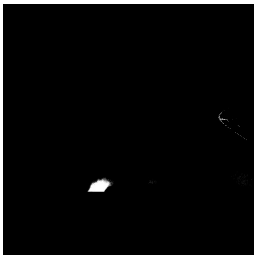

Figure 13: Period 5

Figure 14: Period 6

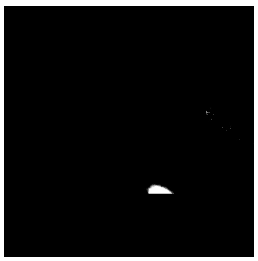

Figure 15: Period 7

Figure 16: Period 8

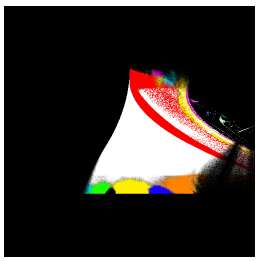

Figure 17: Composition of the above

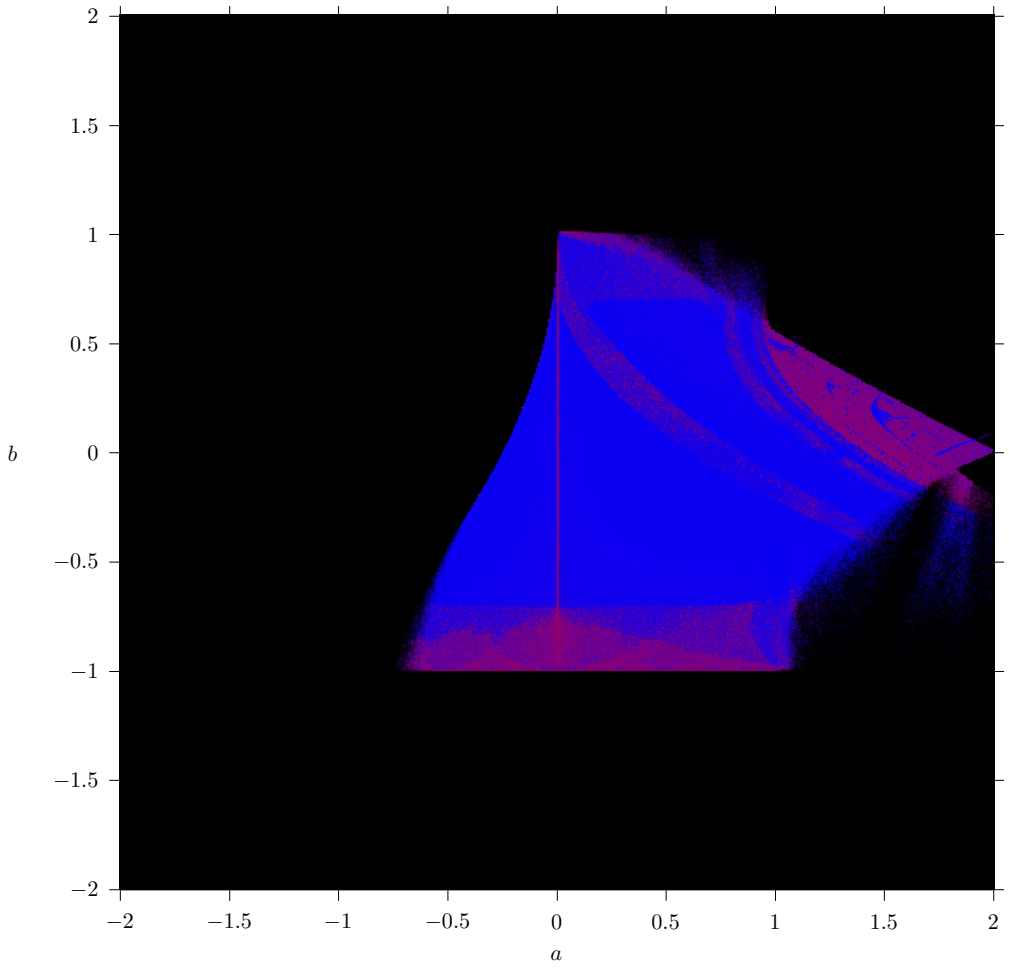


Figure 18: Hénon Lyapunov map

Bright red and purple represent chaotic regions which have no attracting cycles. These are again colored according to the Lyapunov exponent. The brighter the red, the more positive the Lyapunov exponent, and more chaotic the region. Figure 18 is a map which plots just the value of the Lyapunov exponent across the parameter space. Notice that in the areas where there are attracting cycles, the map is much more blue, indicating a negative exponent. One can see that the lower area of the map (around where $b = -1$) has much more red in it, and may have exponents which are positive. The area to the right has exponents which are definitely positive, as this is where the classic Hénon attractor is from.

## 3.7 Geography of the Hénon parameter map

There is a rich variety of behavior and peculiar features in the Hénon parameter map. Let us first make a few general observations before examining individual regions of parameter space in detail. All bounded structures in the parameter

space occur for $-1 \leq b \leq 1$. The entire region in parameter space appears to be bounded on the left by some curve, and partialy bounded on the right by a parabola. I say partially, because there are some pockets of bounded behavior that show up behind the parabola. Most of the parameter space corresponds to maps which are stable; they have strongly attracting structures. Towards the extremities, and also partially under the parabola, the map seems to have a fair bit of chaotic behavior, but these regions seem to be interspersed with stable bubbles or pockets. Towards some of the edges of the map, and also in the area near $(1.5, -0.5)$, the bounded structures in the phase space become thin or move far from the origin, and this causes the nearby areas to take a fuzzy appearance, as a consequence of the random sampling.

Despite this apparent fuzziness in the rendering of the Hénon map, the entire structure does appear to be closed and necessarily compact. The set of parameters that yield bounded structures does not appear to have direct fractal characteristics, but there are small details in the chaotic regions which seem to have a self-similar appearance.

The filled-in Julia-like sets are all plotted for $(x, y) \in [-5, 5] \times [-5, 5]$, unless explicitly marked as a magnification. These sets have a few common factors. They all appear to be bounded by parabolas, and sometimes the set can seem to extend out quite far. Some of these sets may extend towards infinity, though I have not tested for this explicitly. One general feature to note is that above the line $b = 0$, the bounding parabolas tend to open upward, and below the line, the parabolas tend to open downward, this may be attributed to the changing sign of the Jacobian.

In the phase space maps, each point in an image is colored according to the value of the measured Lyapunov exponent and where the point eventually winds up after about 5000 iterations. This coloring scheme did not actually become very useful for providing information about the maps, but it does aid partially in differentiating cycles and the different components of the phase space. In areas where the differences are hard to distinguish, I have sometimes enhanced the images, but it is always indicated when I am doing this.

### 3.7.1 The looping features at the bottom

Looking carefully here, it is possible to see a peculiar branching structure that is not unlike a bifurcation diagram. Towards the bottom of the map, we see that the branching grows thick enough that it becomes interpreted as chaos. As a matter of fact, at the very bottom, on the line $b = -1$, this does become chaotic. The Lyapunov exponents do become greater here, though they stay negative in the areas where there are attracting cycles. If one examines the colors carefully, the periods of the "bubbles" increase as $b$ approaches $-1$. In between these bubbles, there is what would appear to be simultaneous seperate cyclic structures. There is, however, a great deal of granularity here, as in the self-similar black region. It would seem as though this granularity would become explained through examination of the Julia-like sets, but I was not able to observe any real correlation between the grain patterns and the shape of either the attractors or the Julia-like sets. It may also be an artifact of the sampling method, but I was not able to test for this, either. Many of these sets appear as though there is both an (at least) weakly attracting fixed point and a periodic cycle.

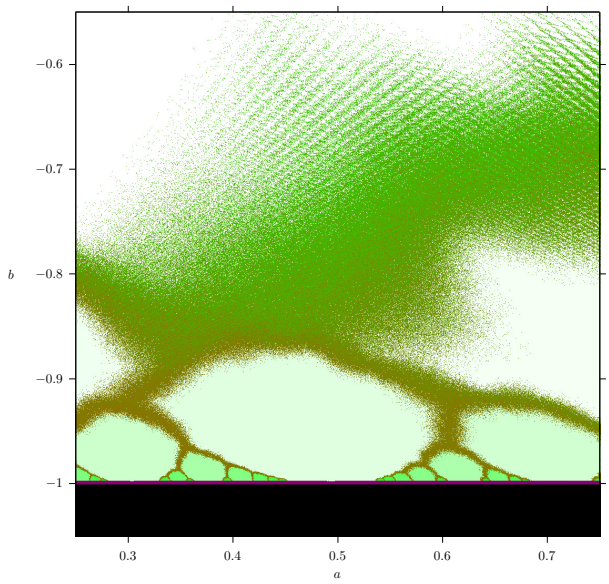


Figure 19:

Figure 20: $(0.85, -0.75)$

Figure 21: $(0.85, -0.99)$

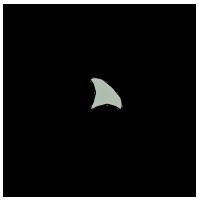

Figure 22: $(0.85, -1.0)$

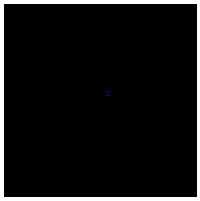

Figure 23: $(0.85, -1.0)$ orbit

Let us examine a few examples in which $b$ becomes close to $-1$.

The images (Figures 20-23) appear to contain a single basin which constricts as $b$ nears $-1$. However, where $b = -1$, it is possible to see a ring of 10 small isolated dots around the main structure. It would seem to be likely that these are the basin of a 10 periodic cycle, since the attractor which lies in the center region does not extend into that area. It also suggests that this 10-cycle exists for greater values of $b$, but may simply be more difficult to see.

In the orbit image, it is possible to see the orbit of the attractor of the central region, though the images have been touched up slightly to make this more visible. It is very interesting to note how the attractor spontaneously becomes a very clear loop. On this loop, the Hénon map is likely to behave akin to an angle doubling map on the unit circle.

It is possible to see in Figures 28-31 that there is a 3-cycle in addition to the central fixed point. However, at $b = -1$, this 3-cycle seems to vanish. It is evident in the parameter map that the bubbles which feature attracting cycles have borders which cross vertical paths as $a$ is fixed. So it should seem perfectly reasonable that a basin of an $n$-cycle can disappear and a basin of an $m$-cycle can begin. Compare this with Figures 24-27, in which the three cycle and central

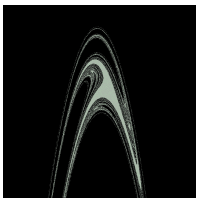

Figure 24: $(1.1, -0.75)$

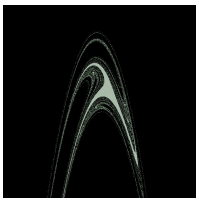

Figure 25: $(1.1, -0.8)$

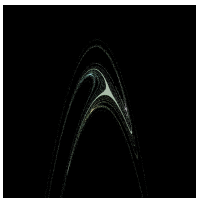

Figure 26: $(1.1, -0.9)$

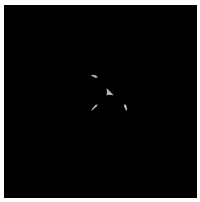

Figure 27: $(1.1, -1.0)$

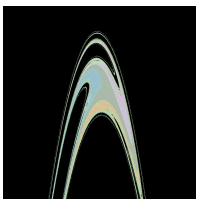

Figure 28: $(1.0, -0.75)$

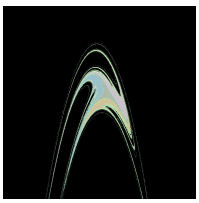

Figure 29: $(1.0, -0.9)$

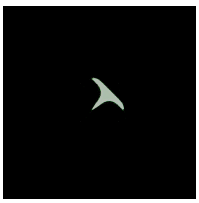

Figure 30: $(1.0, -1.0)$

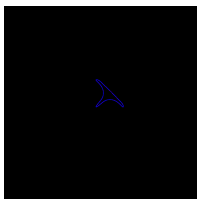

Figure 31: $(1.0, -1.0)$ orbit

point separate as $b$ approaches $-1$.

However, since chaos becomes present at $b = -1$, and some of the bubbles appear to extend all the way towards that line, it would seem likely that some of the Julia-like sets on $b = -1$ will feature multiple chaotic structures. If we push $a$ out a little further, this can be seen to be the case in Figures 32-35. Upon very close investigation, it does appear as though the orbits are somewhat thick, and they may not just be a loop, but have some more elaborate behavior.

There are also other areas which seem to exhibit chaotic behavior in this region even without being at $b = -1$. For example, consider the following images (Figures 36-38) which are at $a = 0.2$. When $b = -0.8$, the map appears to be fairly straightforward. However, when $b = -0.9$, some peculiar structures appear on the inside of the Julia-like set's edges. In the enhanced image, where the contrast is increased to highlight the difference, it is clear that there is a great deal of variation in the color in the regions in the edges, which indicates that the points do not converge to a single cycle. I was unable to plot an orbit in this area, though it would appear to be a chaotic region with 4 components. Unfortunately, this appears to be located in an evidently stable region in the parameter space, so it is unclear what precisely this means.

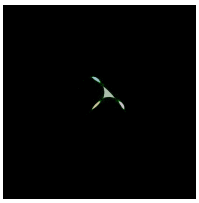

Figure 32: $(1.04, -1.0)$

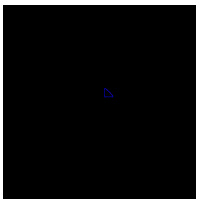

Figure 33: $(1.04, -1.0)$ orbit 1

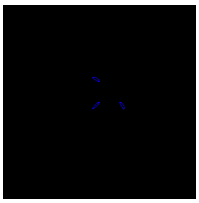

Figure 34: $(1.04, -1.0)$ orbit 2

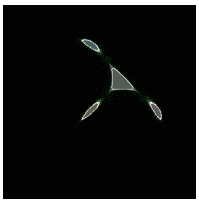

Figure 35: $(1.04, -1.0)$ zoomed overlay

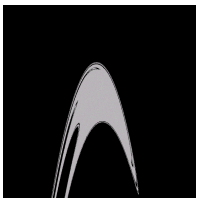

Figure 36: $(0.2, -0.8)$

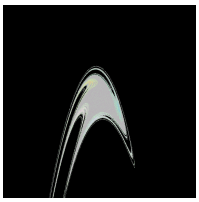

Figure 37: $(0.2, -0.9)$

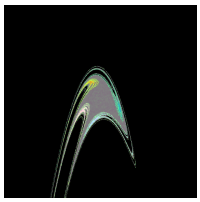

Figure 38: $(0.2, -0.9)$ enhanced

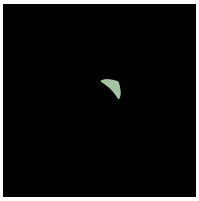

Figure 39: $(2.0, -1.0)$

Figure 40: $(2.6, -1.0)$

Figure 41: $(3.2, -1.0)$

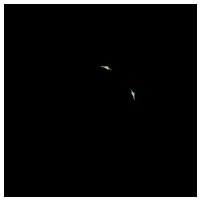

Figure 42: $(3.5, -1.0)$

One characteristic of this area remains especially puzzling, and that is the strange criss-crossing grain patterns in the areas with multiple cycles. This pattern is also reflected in the values of the Lyapunov exponents, so if this pattern is not actually a part of the Hénon map, it must be due to the way cycles are evaluated. I was not able to investigate thoroughly what transitions occured as the parameters move across these regions.

### 3.7.2 The remainder of the panhandle at the bottom

The entire region near $b = -1$ in parameter space continues rather far to the right. I have not determined precisely what the value of $\alpha$ is such that for $a > \alpha$ there are no bounded structures. It would seem clear that such a boundary exists, however it is very difficult to measure because the Julia-like sets become very thin as $a$ increases. To see what kind of difference this makes, consider Figures 39-42.

Towards that extreme end, around where $a = 3.5$, the Julia-like sets become very thin and are fairly hard to measure. The dynamics they exhibit seem to also completely branch in two, so instead of having a cyclic structure around a fixed structure, the fixed structure disappears completely. This is perhaps a result of the fixed point changing from at-least weakly attracting to nonattracting.

Figures 43-46 show a transition decreasing $b$ where $a = 3.5$. In $(3.5, -0.84)$, there appears to be a 6-cycle, which is indicated via the arrows. It is intriguing that despite the Julia-like set losing many recognizeable features when $a$ increases, it nonetheless maintains a complex structure.

### 3.7.3 The looping features at the top

Similar to the area in the bottom of the parameter space, this area also contains higher order cycles and chaotic areas that lie between them. The layout of the

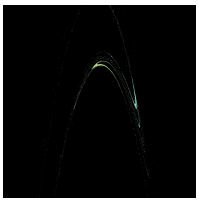

Figure 43: $(3.5, -0.85)$

Figure 44: $(3.5, -0.84)$

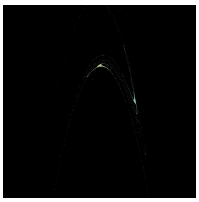

Figure 45: $(3.5, -0.9)$

Figure 46: $(3.5, -0.99)$

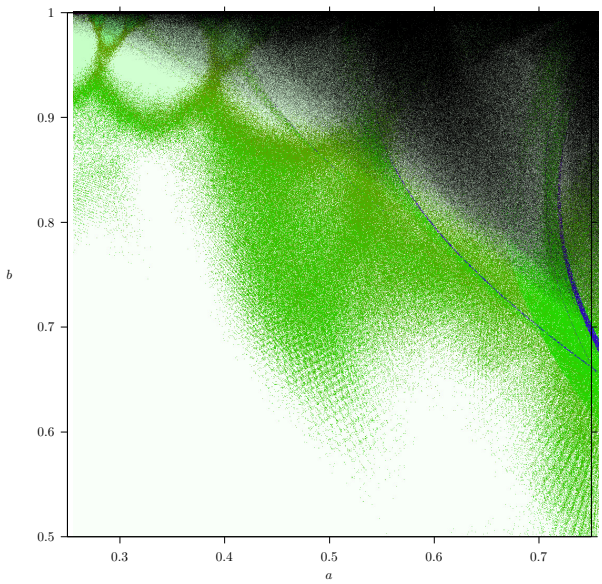


Figure 47: Zoom of the top of the Hénon parameter map

Figure 48: $(0.2, 0.85)$

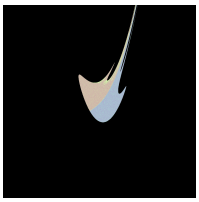

Figure 49: $(0.2, 0.90)$

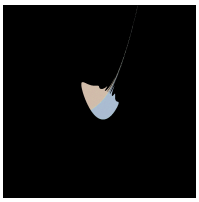

Figure 50: $(0.2, 0.99)$

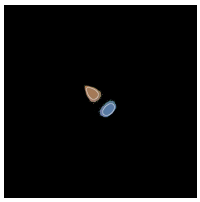

Figure 51: $(0.2, 1.0)$

Figure 52: $(0.3, 0.999)$

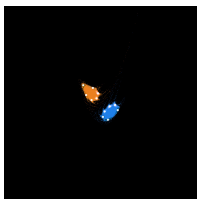

Figure 53: $(0.3, 0.999)$ enhanced

periodic bubbles is slightly different, but they still appear to divide as they reach the edge of the parameter space, this time near $b = 1$. This region is much tighter than along $b = -1$. The edge of parameter space touching $b = 1$ begins at $a = 0$ and appears to end around $a = 1.25$. Compare this with the edge near $b = -1$, which contains the same type of branching structure and is likely to express dynamics which are just as diverse. The Julia-like sets in this region also exhibit a very interesting feature different from those near $b = -1$; they all appear to have two parts. The bounded structures in the Julia-like sets appear to have reflections across a quadratic curve. The periods of the stable cycles are multiples of two and the chaotic structures also get reflected between two separate components (Figures 48-51).

When $b$ was near $-1$, there was a trend for there to be a single fixed point, around which a cycle would orbit. This trend also seems to continue here, but instead of the cycle orbiting around a fixed point, it orbits around a 2-cycle. For example, in Figures 52 and 53, the first image appears to be a simple reflecting two cycle. However, it also happens to have a 12-cycle spinning around it, as shown in the enhanced version next to it. I would attribute this duality to the fact that when $b > 0$, the Jacobian for the Hénon map is negative, and thus creates flip-flopping behavior. If this is indeed the case, then it is unlikely that we will find areas whose foci are three cycles are more.

We can observe this trend continue in the sets where $b = 1$ (Figures 54-57).

### 3.7.4 The bright chaotic region in the upper right, and the pockets of stability within

This is where the typical folded Hénon map $(1.4, 0.3)$ comes from. However, that is by far not the most interesting coordinate in the parameter space in this portion of the map. Some very peculiar parts of the parameter space manifest themselves here, where stable pockets reach out beyond the unstable

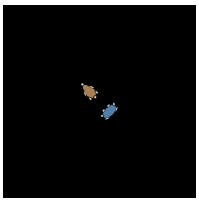

Figure 54: $(0.3, 1.0)$

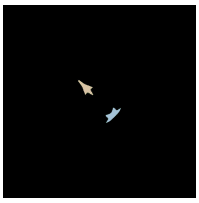

Figure 55: $(0.5, 1.0)$

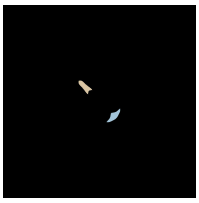

Figure 56: $(0.6, 1.0)$

Figure 57: $(1.0, 1.0)$

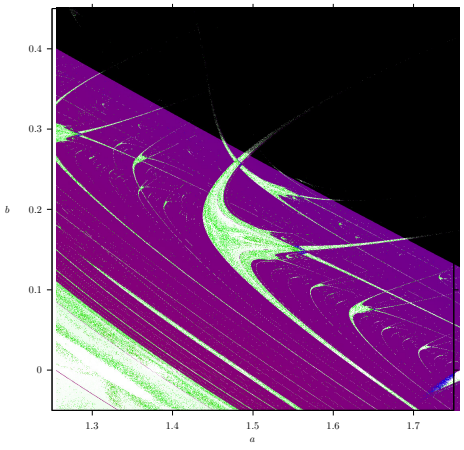


Figure 58:

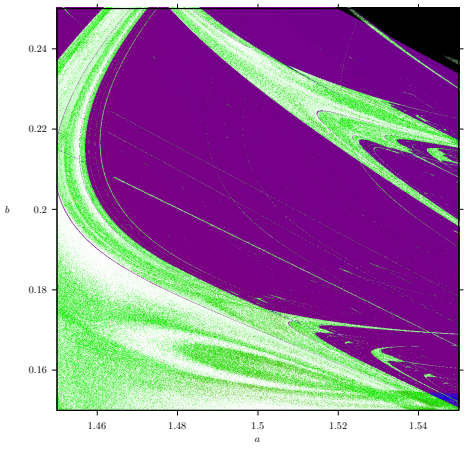


Figure 59:

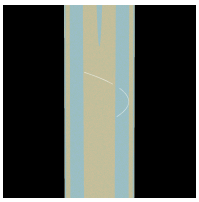

Figure 60: $(1.5, 0.01)$

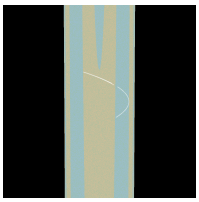

Figure 61: $(1.5, 0.02)$

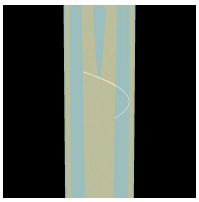

Figure 62: $(1.5, 0.03)$

Figure 63: $(1.5, 0.04)$

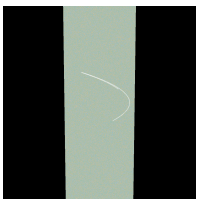

Figure 64: $(1.5, 0.05)$

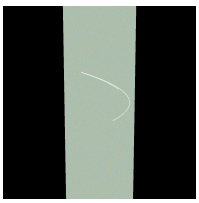

Figure 65: $(1.5, 0.06)$

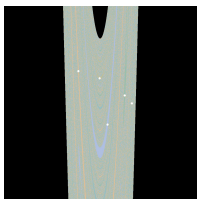

Figure 66: $(1.5, 0.10)$

black border, sometimes curving around and returning. These small pockets of stability also are preserved in the chaotic region.

Investigating closely, threads of stability appear to be interspersed amidst the chaos, and it is likely that they are in fact dense. These threads also cross each other, and occasionally merge together in small clusters. It is difficult to observe what precisely occurs when the stable threads overlap each other, but it seems that if a thread of period $m$ overlaps a thread of period $n$ then either both periods will coexist, or there will be a pocket where the period is $mn$. Due to the very fine nature of these structures, I was not able to test this explicitly.

This particular space is rich in patterns; consider Figures 60-66 where $a$ is fixed at 1.5 and $b$ is varied between 0 and 0.1. Initially the attractor is in two separate parts which move closer together, and these separate parts can be observed quite clearly in the phase space. When they meet, the two regions of the Julia-like set in the phase space merge into one and become indistinguishable.

The last image, at $(1.5, 0.1)$, features a periodic cycle. When the parameters are varied, the period and the points change, but they stay on the same general curve, as we can see in Figures 67-70.

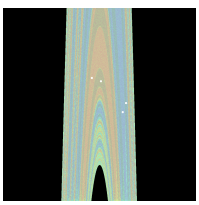

Figure 67: $(1.5, -0.1)$

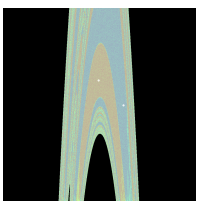

Figure 68: $(1.5, -0.2)$

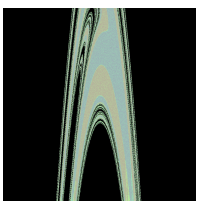

Figure 69: $(1.5, -0.3)$

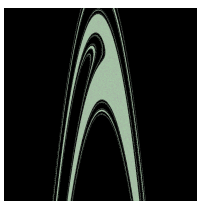

Figure 70: $(1.5, -0.5)$

Figure 71: $(1.28, 0.58)$

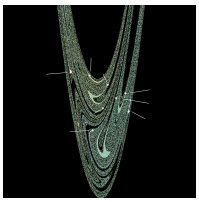

Figure 72: $(1.08, 0.52)$

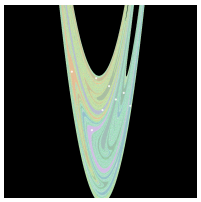

Figure 73: $(1.02, 0.48)$

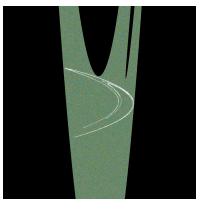

Figure 74: $(1.4, 0.3)$

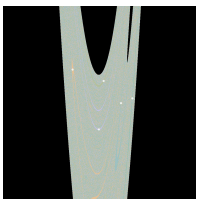

Figure 75: $(1.47, 0.252)$

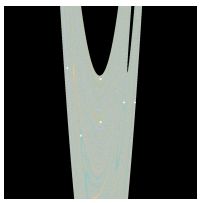

Figure 76: $(1.474, 0.258)$

Many other peculiar features occur within the bubbles in the parameter space. When the periodic areas jut out into the divergent area, the Julia-like sets become very narrow and hard to detect. The following images contain cycles with very tiny basins of attraction. The actual points in the cycles are highlighted. Their narrowness raises the question of how far these stable threads extend out into the unstable region of parameter space until they disappear entirely (Figures 71-73).

It is possible to see some periodic behavior near the classic Hénon map. Figure 74 contains the classic Hénon map and Figures 75 and 76 contain slight perturbations in which the chaotic attractor degenerates into a cycle.

### 3.7.5 The line $b = 0$

In this, the simplest of cases, The two dimensional map becomes the map $x_{n+1} = 1 - ax_n^2$. However, this map is also conjugate to $x_{n+1} = -a + x_n^2$. This is a very familiar map when the variables are complex. In our map we are only considering the real coordinate, but superimposing the Mandelbrot set on the Hénon parameter space yields a surprising discovery (Figure 77).

This is not a new observation, as the Henon map has been examined in the complex plane with a fair amount of detail [28]. Nonetheless, it is intriguing to see the interaction between the two dissimilar mathematical structures.

Here, we see why much of the region underneath the purple quadratic arch is necessarily of period 1, and why a lot of the region above it is of period two. Looking carefully, it is possible to see purple lines that intersect where the bulbs of the Mandelbrot set separate on the axis. Additionally, the spaces where there are "mini" Mandelbrot sets overlay regions which have periodic behavior. Since we know that the Mandelbrot set is connected, and thus the mini-Mandelbrots are as well, it appears to be the case that there are infinitely many stable periodic strips throughout the chaotic region.

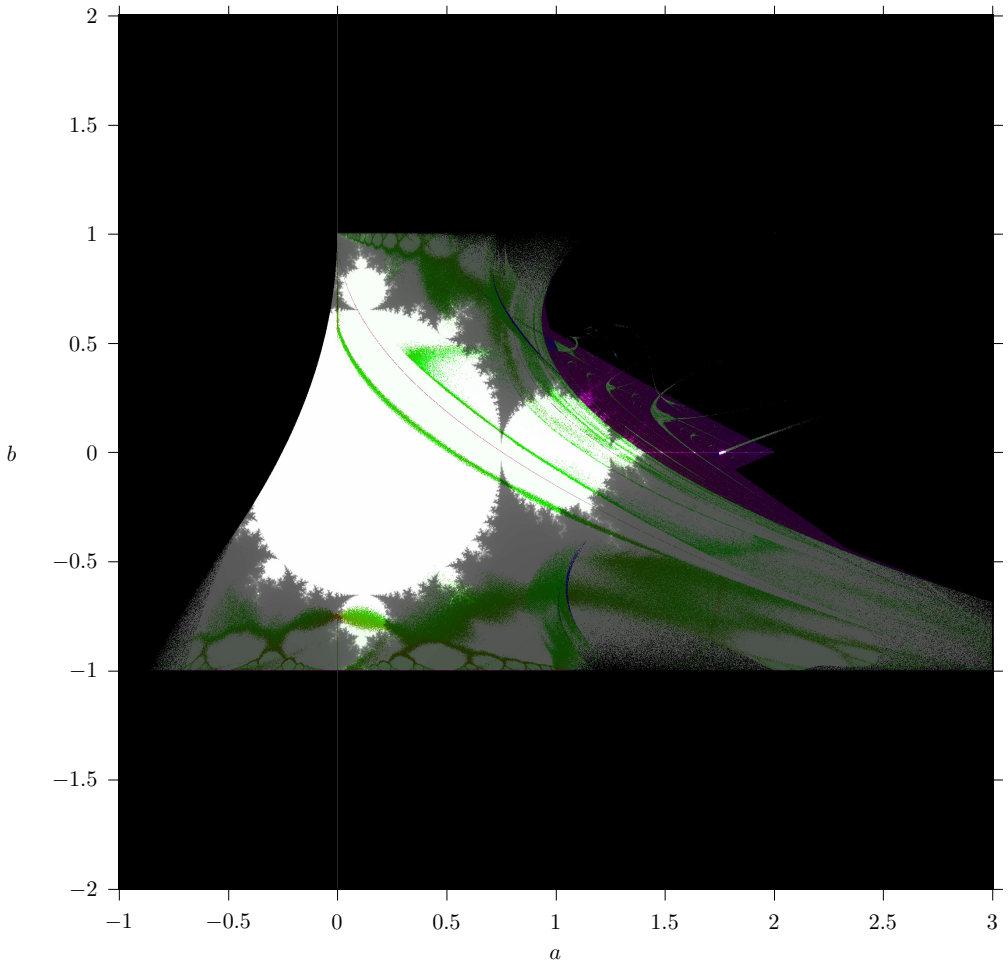


Figure 77: Superimposition of the Mandelbrot set.

### 3.8 Fractal behavior in parameter space

Some of the patterns in the Hénon parameter map clearly have self similar structure, but is it possible to show that this is actually a fractal? This question is complicated, because the boundary of the stable region of the parameter space is hard to plot out numerically, although many of the boundaries do seem to be smooth. There do appear to be unmistakably self similar features sprinkled throughout the parameter space. Much like there are lobes on the Mandelbrot set which describe parameterizations that contain periodic components of certain degrees. There are also recognizable regions which dictate the period and structure of the orbits under those parameters, as well as the shape and behavior of the Julia-like sets as well.

These sets of parameters do not appear to have fractal dimension themselves, but their borders may, and the pockets of stability in the chaotic region of the Hénon parameter map appear to be procedurally "generated" somehow, such as through a nonlinear iterated function system.

## 4 Lessons Learned from Complex Analysis

Most of the knowledge we have regarding fractals originates from studying conformal maps iterated on the complex plane. The conformality of complex mappings makes the analysis of dynamics very straightforward. Despite the fact that $\mathbb{C}$ has two dimensions, it behaves in a one dimensional manner under conformal mappings; as a result, dynamics in $\mathbb{C}$ will be very different than the dynamics in $\mathbb{R}^2$. Nonetheless, there are several important concepts from complex analysis that would be beneficial to address here in order for us to draw a few analogies between the two types of systems.

### 4.1 Types of fixed points and their behavior

The dynamics of a system $f \in \mathbb{C} \to \mathbb{C}$ depend very heavily on the properties of the fixed points. From these we can get a good understanding of the coordinate systems under $f(\mathbb{C})$. A fixed point $z_0$ falls into one of three categories dependent its derivative $f'(z_0)$. The fixed point is attracting, neutral, or repelling if the norm of the derivative is less than one, equal to one, or greater than one respectively.

For rational functions of degree $d$, the number of critical points (points at which $f'(x) = 0$) is bounded by $2d - 2$. The number of attracting cycles on $\hat{\mathbb{C}}$ is bounded by the number of critical points. Through further analysis, it is also possible to place bounds on the number of neutral fixed points, and there is a bound of $6d - 6$ on the number of attracting and neutral fixed points [2].

Additionally, cycles may be classified in a manner similar to fixed points. For ease of notation, let us represent iterates of functions with superscripts, so that $f(f(z)) = f^2(z)$, and $f \circ f^n = f^{n+1}$. The derivative of a cycle $z_1, z_2, \ldots, z_p$ of period $p$, is $(f^p)'(z)$ taken at any of the points on the cycle. Using the chain rule, we have a handy formula:

$$\begin{aligned}(f^p)'(z_1) &= (f^{p-1} \circ f)'(z_1) \\ &= (f^{p-1})'(f(z_1))f'(z_1) \\ &= (f^{p-1})'(z_2)f'(z_1) = \prod_{k=1}^{p} f'(z_k)\end{aligned}$$

Cycles may also be described as attracting, repelling, or neutral, depending on the norm of the derivative. Also note that the above rule is applicable to any dynamical system in which the chain rule holds, not only for conformal systems.

## 4.2 Mandelbrot and Julia sets

Under a rational map, the complex plane is divided into two parts. There is the Fatou set on which the eventual behavior of points under the map is predictable. This set consists of attracting fixed points and cycles, as well as their basins, as well as points which diverge to infinity. In complex analysis, infinity may simply be regarded as a single point in the Riemann Sphere, and for, polynomials, an unbounded sequence may be thought of as just approaching the fixed point of infinity. There is the Julia set, which contains the repelling cycles and all the points that are unpredictable or chaotic.

Julia sets are the borders of the basins of attraction in complex dynamical systems. The filled-in Julia set is the compliment of the basin of attraction of infinity. For a polynomial, the Julia set may be either connected or totally disconnected. Most of the time, we will only be concerned with the map $z^2 + c$, and the connectivity of the Julia set depends on the behavior of the iterates of the function at the point 0. If the iterates are bounded, then the Julia set is connected, otherwise it is totally disconnected. The Mandelbrot set $\mathcal{M}$ is the set of all $c$ such that $J_c$ is connected. As such, the $\mathcal{M}$-set is essentially a map of the parameter space for all possible Julia sets for a given parameterizable function, and is commonly referred to as the connectivity locus for this reason.

The function with the most studied Julia sets is the classical quadratic function $z^2+c$. Of crucial importance in the study of the Julia sets of this polynomial is the forward orbit of the critical point 0. This orbit and its limit set, if it has one, describes in general the overall structure of the Julia set. For $c \in \mathcal{M}$, the limit set of the orbit of 0 is the attracting cycle for all points in the interior of the filled in Julia set. When $c$ is chosen in any of the bulbs of the Mandelbrot set, the orbit of 0 tends to an attracting cycle whose period is determined by the combinatorial arrangement of the bulb's placement in the $\mathcal{M}$-set.

## 4.3 External Rays and Symbolic Dynamics

The strange combinatorial structure of the Mandelbrot and Julia sets may be described through symbolic dynamics as illustrated by Keller and Olivia in [13, 14, 26]. Symbolic dynamics hinges on the interpretation of equivalences and conjugations in dynamical systems.

These symbolic techniques can be used to lay out the similarities and equivalences in the dynamics of the Julia sets for every value of $c$. The systems of equivalences in dynamics are called invariant factors. When there exist conjugations between dynamical systems, the systems may be thought of as equivalent.

It is possible to separate all the dynamical systems that arise from the functions $f_c$ into equivalence classes based on these conjugations. This type of analysis works particularly well in the conformal case of complex dynamics, but it also is relevant in the non conformal case, when we are trying to distinguish between different systems.

External rays are a helpful combinatorial tool in analyzing Julia sets. The following is paraphrased from Olivia [26], who provides a very straightforward explanation of external rays. When a Julia set is connected, its topology may be projected onto a circle. We may describe a bijection $\phi_c \in \mathbb{C} - J \to \mathbb{C} - \overline{\Delta}$, which conjugates the dynamics of $f_c$ outside the filled in Julia set $K_c$ to the behavior of $z \mapsto z^2$ outside of the unit disk. This conjugation should actually be fairly intuitive, as in both dynamical systems, all points chosen will iterate towards infinity. The notion of external rays comes from taking the rays originating from the unit disk to infinity and examining their projections under $\phi^{-1}$. For example, a ray with angle $\theta$ lands at $z_\theta$ if $z_\theta = \lim_{r \to 1} \phi^{-1}(r\mathrm{e}^{\mathrm{i}\theta})$. The landing lemma of Douaday and Hubbard states that rays with rational angles always land. When the extension of $\phi^{-1}$ is continuous on the unit circle, the landing map $\theta \mapsto \phi^{-1}(\mathrm{e}^{2\pi\mathrm{i}\theta})$ forms a semi-conjugacy from the angle doubling map on the unit circle to $f_c$ on $J_c$. The unit circle and the doubling map is also semi-conjugate to right-infinite binary sequences and the left shift map. The conjugation to this system provides a combinatorial model of $J_c$ as a quotient of the space of binary sequences.

We have seen this sort of angle doubling behavior before in the Hénon phase maps, where the limits of the attractors at $b = -1$ formed loops. It is imaginable that the analysis of external rays could be applied quite neatly to those maps, since the Julia-like sets were connected and had only one component. The analysis of external rays falls apart in some other situations where the basins of attraction for the system form several disconnected components. This occurs because there is no natural mapping $\phi \in \mathsf{X} - J \to \mathsf{X} - \overline{\Delta}$, which is obviously invertible. It would be conceivable to form some kind of analogue, though, and such analysis may prove to be fruitful.

## 4.4 Continuity of Julia sets under variation of parameters

Under certain conditions, it is a significant question whether the map $c \mapsto J_c$ is continuous under the Hausdorff metric. This problem was first posed by Douady [27], and affirmed for the polynomial case. Several details of this continuity is discussed by Kriete in [16, 17, 18], who illustrates instances of the Julia set for a sequence of functions converging or not. It remains to be seen whether claims may be made for continuity under parameterizations, particularly for the case when the function is differentiable with respect to its parameter.

Suppose a sequence of functions $\{f_d\}_{d \in \mathbb{N}}$ converges uniformly on compact sets to a function $f$. Also suppose that these functions are meromorphic on $\mathbb{C}$, that is, $f(z) = g(z)/h(z)$, where $g$ and $h$ are entire and $h$ is nowhere zero. Then, it is possible to show that the Julia sets $J(f_d)$ converge to $J(f)$ in the Hausdorff metric, if the Fatou set $F(f)$ is the union of the basins of attracting periodic orbits and $\infty \in J(f)$. The following is a sketch of the proof given in [17]:

Using the chordal metric in the Riemann sphere, $\hat{\mathbb{C}}$, recall that the Hausdorff

distance, $h(A, B)$, is defined as:

$$h(A, B) = \inf\{\epsilon > 0 \,|\, A \subset V_\epsilon(B), \text{ and } B \subset V_\epsilon(A)\}$$

Where $V_\epsilon(X)$ is the $\epsilon$-neighborhood of $X \subset \hat{\mathbb{C}}$.

First, let $O(z_0)$ be the orbit of an attracting or repelling cycle of period $k$ in $f$. For some $N \in \mathbb{N}$, $f_d$ has a respectively attracting or repelling $k$-periodic orbit $O(z_d)$ for all $d > N$. Additionally, $O(z_d)$ converges to $O(z_0)$ in the Hausdorff metric. Also, if $A(z_0)$ is the basin of $O(z_0)$, for every compact $K \subset A(z_0)$, there is an $N \in \mathbb{N}$, such that $K \subset O(z_d)$ for all $d > N$. It has been shown in Hirsh and Smale [29] that a $k$-periodic orbit (and its basin if it is attracting) will persist under small $C^1$ perturbations of the function.

To show the Hausdorff convergence of Julia sets, we note that since $\infty \in J(f)$, the Fatou $F(f)$ set consists of the basins of attracting periodic orbits $O(z_i) \subset \mathbb{C}$. Let $\epsilon > 0$, and define $F^\epsilon(f)$ as $\hat{\mathbb{C}} - V_\epsilon(J(f))$. This is compact in $\hat{\mathbb{C}}$ and it must intersect only finitely many $A(z_i)$. Therefore there must exist $N \in \mathbb{N}$ such that $F^\epsilon(f) \subset F(f_d)$ for all $d > N$. Additionally, $J(f_d) \subset V_\epsilon(J(f))$. To see that for large enough $d$, let $w \in J(f)$. Since repelling periodic points are dense in $J(g)$, let $z_0 \in V_\epsilon(w)$, as a repelling periodic point of $f$ with period $k$. Then we know that there is another $k$-periodic orbit for $f_d$, $O(z_d)$ which converges to $O(z_0)$. Since $O(z_d)$ lies in $J(f_d)$, the arbitrarily chosen point $w$ lies in $V_\epsilon(J(f_d))$. And this is enough to show the other side of the Hausdorff convergence, since $J(f)$ is compact.

Of course, there are important situations that do not satisfy each of these conditions. Specifically, the condition where $\infty \in J(f)$ is significant and easy to overlook. Kriete explores situations when the continuity in question is analyzed by taking the limit of arbitrary sequences of Julia sets. If we take the sequence of functions $f_d$, which are governed by a sequence of parameters $c_d$, where $f$ is differentiable with respect to $c$; it is conceivable that there may be some regions in the parameter space where the Julia set is continuous. After all, both attracting and repelling cycles are preserved under small perturbations of the function.

We have seen the kinds of changes that occur in the Hénon Julia-like sets when parameters are perturbed only slightly. Even though the period sometimes changes, the shape of the filled-in Julia-like set tends to be mostly preserved, and when the parameters are varied away from the divergent regions, the filled-in Julia-like sets appear to be continuous with respect to the parameters. Kriete proves that filled-in Julia sets are continuous with respect to the Hausdorff metric [18], so it is not too far of a stretch to suppose that filled-in Julia-like sets are continuous for certain conditions as their parameters are varied.

# 5 Application to Differential Equations

Dynamics in differential equations tend to be more commonly studied than in discrete systems, but there are a number of dynamical properties that are shared by both systems. It is good to address some of these properties in the continuous case for the purpose of making analogies. Continuous systems tend to be better behaved than discrete systems because they may not wildly skip across the phase space, like discrete systems are prone to doing. In fact, if the continuous system is planar, then chaotic behavior cannot even occur.

## 5.1 Stability under perturbation of initial point

Let us consider an ordinary differential equation (ODE) of the form:

$$\dot{\boldsymbol{x}} = f(t, \boldsymbol{x})$$

Where $f \in C^1(\mathbb{R} \times \mathbb{R}^N \to \mathbb{R}^N)$, and $\dot{\boldsymbol{x}}$ represents $\frac{\mathrm{d}}{\mathrm{d}t}\boldsymbol{x}(t)$.
Supposing that $f$ obeys a Lipschitz condition, continuous variation of the initial point $\boldsymbol{x}_0$ produces a continous variation of the curve of the ODE starting at $\boldsymbol{x}_0$. More precisely, if $\boldsymbol{x}(t)$ represents $\boldsymbol{x}$ at time $t$, then $\boldsymbol{x}_0 \mapsto \boldsymbol{x}(t) \in \mathbb{R}^N \to \mathbb{R}^N$ is a continuous function.

If on some convex $D \subseteq \mathbb{R} \times \mathbb{R}^N$,

$$\|f_{,\boldsymbol{x}}(t, \boldsymbol{x})\| \leq B, \text{ where } (t, \boldsymbol{x}) \in D$$

We may derive a Lipschitz condition:

$$\|f(t, \boldsymbol{x}_2) - f(t, \boldsymbol{x}_1)\| \leq B\|\boldsymbol{x}_2 - \boldsymbol{x}_1\|$$

Recalling again the little-oh notation, by Taylor's theorem, we have:

$$f(t, \boldsymbol{x}_2) - f(t, \boldsymbol{x}_1) = f_{,x}(t, \boldsymbol{x})(\boldsymbol{x}_2 - \boldsymbol{x}_1) + o(\|\boldsymbol{x}_2 - \boldsymbol{x}_1\|)$$

Now, let us examine the variational system for the solution $\boldsymbol{x}(t; t_0, \boldsymbol{x}_0)$, which is a matrix ODE defined by the following:

$$\dot{\boldsymbol{X}} = f_{,\boldsymbol{x}}(t, \boldsymbol{x}(t; t_0, \boldsymbol{x}_0))\boldsymbol{X}(t), \text{ and } \boldsymbol{X}(t_0) = \boldsymbol{I}$$

This system has a unique solution:

$$\boldsymbol{X}(t; t_0, \boldsymbol{I}) = \mathbf{exp}\left(\int_{t_0}^{t} f_{,\boldsymbol{x}}(s, \boldsymbol{x}(s; t_0, \boldsymbol{x}_0))\,\mathrm{d}s\right)$$

Given $(t_0, \boldsymbol{x}_1)$ and $(t_0, \boldsymbol{x}_2)$ in $D$, we may show that the solutions $\boldsymbol{x}(t; t_0, \boldsymbol{x}_1)$ and $\boldsymbol{x}(t; t_0, \boldsymbol{x}_2)$ (subsequently referred to as $\boldsymbol{x}_1(t)$, and $\boldsymbol{x}_2(t)$, respectively) are close when $\|\boldsymbol{x}_2 - \boldsymbol{x}_1\|$ is small.

$$\boldsymbol{x}_1(t) = \boldsymbol{x}_1 + \int_{t_0}^{t} f(s, \boldsymbol{x}_1(s))\,\mathrm{d}s,$$

which may be applied for both $\boldsymbol{x}_1$ and $\boldsymbol{x}_2$, so:

$$\boldsymbol{x}_2(t) - \boldsymbol{x}_1(t) = \boldsymbol{x}_2 - \boldsymbol{x}_1 + \int_{t_0}^{t} f(s, \boldsymbol{x}_2(s)) - f(s, \boldsymbol{x}_1(s))\,\mathrm{d}s$$

Making use of the Lipschitz condition and Gronwall's inequality, we can obtain the bound:

$$\|\boldsymbol{x}_2(t) - \boldsymbol{x}_1(t)\| = \|\boldsymbol{x}_2 - \boldsymbol{x}_1\|\mathrm{e}^{B(t-t_0)}$$

furthermore,

$$\boldsymbol{x}_2(t) - \boldsymbol{x}_1(t) = \boldsymbol{X}(t; t_0, \boldsymbol{I})(\boldsymbol{x}_2 - \boldsymbol{x}_1) + o(\|\boldsymbol{x}_2 - \boldsymbol{x}_1\|)$$

This means that the solutions of the ODE are continuous and moreover differentiable with respect to the initial conditions. (Of course the Lipschitz condition is highly necessary here.)

An interesting observation is that the argument of continuity with respect to initial conditions holds when taking into consideration only some components of $\boldsymbol{x}$. If some components are bound to the Lipschitz condition, and all others held fixed, the same conclusion still applies. This technique does not allow us to improve the claims on differentiability or continuity, but it vastly expands the range in which the claims of differentiability can be made, with respect to those specific initial conditions. For example, if $\|f_{,\boldsymbol{x}_n}(t,\boldsymbol{x})\| \leq B$, then we are guaranteed differentiable continuity with respect to $\boldsymbol{x}_n$, regardless of $f$'s dependence on the rest of the initial conditions.

## 5.2 Stability under perturbation of parameters

Given the very straightforward results regarding initial conditions that ODEs obey, one simple way of handling parameters in an ODE based dynamical system is to embed the parameters into initial conditions. Suppose we are working with an $n$ dimensional system with $m$ parameters. Let $\boldsymbol{x}_0 \in \mathbb{R}^N$, and $\boldsymbol{a} \in \mathbb{R}^M$. We may define $g \in \mathbb{R} \times \mathbb{R}^N \times \mathbb{R}^M \to \mathbb{R}^N \times \mathbb{R}^M$, such that $g(t,\boldsymbol{x},\boldsymbol{a}) = f_{\boldsymbol{a}}(t,\boldsymbol{x})$, and $g(t,\boldsymbol{x},\boldsymbol{a})_k = 0$ for $k > n$. It should be evident that any solution $x_a(t;t_0;\boldsymbol{x}_0)$ of $\dot{\boldsymbol{x}} = f_{\boldsymbol{a}}(t,\boldsymbol{x})$ implies $y = (\boldsymbol{x},\boldsymbol{a})$ is necessarily a solution of $\dot{\boldsymbol{y}} = g(t,\boldsymbol{y},\boldsymbol{a})$.

Using this equivalence, we may make claims regarding the continuity of solutions with respect to parameters; namely that if the initial conditions are fixed, then the solution may be continuous with respect to the parameters.

For example, consider the Riccati system.

$$\dot{x} = a + bx^2$$

This is a system of one variable and two parameters, but may be rewritten as a system of three variables:

$$\begin{aligned} \dot{x} &= a + bx^2 \\ \dot{a} &= 0 \\ \dot{b} &= 0 \end{aligned}$$

Examining specifically the partials with respect to $a$ or $b$, we find that $g_{,a}(t,[x,a,b]) = 1$, and $g_{,b}(t,[x,a,b]) = x^2$, both are respectively constant. This means that the mapping: $(a,b) \mapsto x(t;t_0,[x_0,a,b])$ is continuous and differentiable. Moreover, this holds regardless of $x_0$ or $t_0$.

In this particular case, the reason why this works out so easily is because $f$ is linear with respect to its parameters. Fortunately, most reasonable parameterizations will be linear. Furthermore, if one wishes to have $f$ dependent on both a parameter $a$ and some function of $a$, say $a^2$, it is always possible to introduce a second linear parameter called $b$ which has that value at all times.

## 5.3 Planar systems

Let us examine what can be concluded if the system is planar ($n = 2$). The treatment of fixed points and periodic orbits is fairly well studied in this case,

and many results (particularly the Poincare-Bendixson theorem) highlight conditions for the existence and behavior of such points and cycles. Unfortunately, since a parameter-embedded system will almost certainly have more than two dimensions, the theorems will be difficult to apply directly. Indeed, with certain systems, one may observe situations where an attracting fixed point varies in between a repelling one or a saddle point, and different fixed points may merge or even disappear altogether.

Consider the system:

$$\begin{aligned} \dot{x} &= \alpha x - y \\ \dot{y} &= x + \alpha y \end{aligned}$$

When $\alpha$ is varied, the solution of this system changes from logarithmic spirals originating from the origin ($\alpha > 0$), to concentric circles ($\alpha = 0$), to spirals converging towards the origin ($\alpha < 0$). While each solution originating from some specific condition is itself continuous with respect to $\alpha$, the A and $\Omega$ limit sets have some very clear discontinuity at $\alpha = 0$.

We can see disappearing fixed points in the following system:

$$\begin{aligned} \dot{x} &= x^2 + \alpha - y \\ \dot{y} &= x^2 + \alpha + y \end{aligned}$$

Here, there are fixed points where the curve $x^2 + \alpha$ intersects the $x$ axis. For $\alpha > 0$, they disappear entirely (at least in the real plane). For $\alpha = 0$, there is a saddle point with (seemingly) one positive eigenvalue, and the other zero. For $\alpha < 0$, there is one saddle point and one repelling point.

The behavior of periodic systems under parameters is highly studied. Jack Hale discusses a frictionless pendulum system in [30], and demonstrates how the system subtly changes when damping is applied. In this case the solutions behave in a much more predictable manner, where all the fixed points remain unchanged in terms of their location, but some fixed points transition from neutral to attracting to repelling, exactly as in the case of the spirals above.

For simple linear cases, the roles of fixed points have been extensively discussed in terms of their eigenvalues, and the variation of parameters only yields changes in these eigenvalues, and thus it is not difficult to see what happens when a particular parameter is changed. However, in nonlinear systems, we will be subject to situations akin to the merging and vanishing fixed points.

## 5.4 Strange attractors in ODEs

One can always draw a Jordan curve in a two dimensional system and examine the paths of solutions across the curves. Examining these traversals can reveal locations of fixed points and other properties of the system. In higher dimensions, it is not possible to do this, and things become much more complicated. Trajectories that seem contained around a specific locus may escape that locus and drift off to another one. These sorts of systems tend to be strange attractors, which exist in continuous systems as well. Strange attractors are also defined to be chaotic when nearby initial points separate. The most celebrated strange attractors in continuous systems are Lorenz's weather model, and the Rossler attractor. Despite having the smoothness associated with differential

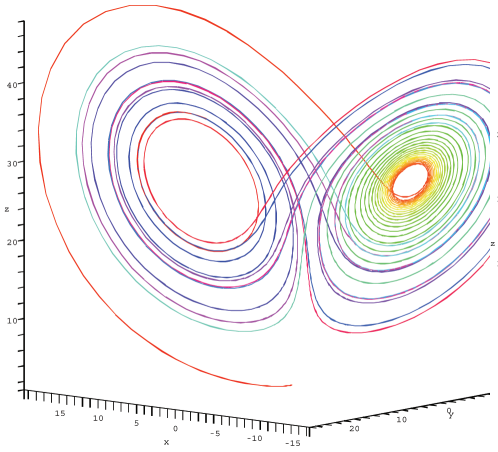

Figure 78: Lorenz Attractor.

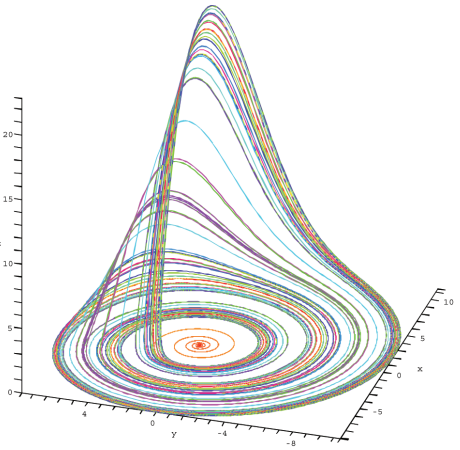

Figure 79: Rossler Attractor.

equations, these systems still manage to have the unpredictable nature that is associated with discrete systems.

In order to behave so unpredictably, the Lorenz and Rossler systems must necessarily be nonlinear, but they are not tremendously nonlinear. They often contain only one or two nonlinear terms, but this is enough to generate tremendously complex dynamics.

Lorenz system:

$$\begin{aligned} \dot{x} &= \sigma(y - x) \\ \dot{y} &= \rho x - y - xz \\ \dot{z} &= xy - bz \end{aligned}$$

Rossler system:

$$\begin{aligned} \dot{x} &= -y - z \\ \dot{y} &= x + ay \\ \dot{z} &= b + zx - cz \end{aligned}$$

The Lorenz system was originally derived from a model of atmospheric convection by Edward Lorenz in 1960. What started out as an exercise in building a more predictable weather model soon became a famous testament to the unpredictability of the weather. The most common representation of the Lorenz attractor features the parameterization: $\sigma = 10$, $\rho = 28$, $b = 8/3$. This produces the classical butterfly-shaped orbit, with two main loops about which orbits can rotate. A minute perturbation in starting conditions however, can drive two orbits to rotate about separate nodes. There do exist cyclical orbits which circle the left and the right nodes in every combination of sequences. The peculiar nature of these orbits led to the term "Strange Attractor", which is a wonderfully appropriate description of these kinds of systems.

The fragile dependence on initial conditions also led Lorenz coin to the famous phrase often used to explain chaos, the "butterfly effect", that "The flap of a butterfly's wings in Brazil could set off a tornado in Texas".

While the Lorenz system is very well known, it is only one of many significant examples of strange attractors that have been discovered in examination of real systems. Another system of interest is the Rossler attractor, discovered by Otto Rossler [22] in 1976 through examination of chemical kinetics. This particular system exhibits something resembling the kneading behavior that is common in quadratic discrete systems. The system appears to resemble a Möbius shape, with ribbons of the orbits folded back into the main loop at every half twist. Typically the Rossler system is parameterized with: $a = 0.2$, $b = 0.2$, $c = 5.7$.

Both of these systems are stable (inasmuch as the orbits will not spin off towards infinity) regardless of initial points. Choosing points that are far away from the origin tend to have the effect of adding "energy" into the system, in that the paths will tend to orbit the foci at a great distance, but they will never diverge to infinity. It is a matter of curiosity if there do exist continuous systems for which some initial points necessarily diverge where others would not, forming Julia-like sets for the continuous systems.

## 5.5 Dimension in Strange Attractors

The orbits of strange attractors, interestingly enough, are fractals and have fractal dimension. Because of the generally nonterminating nature of the orbits, the curves take up a lot of room and can appear to describe a two dimensional surface in three dimensional space. As it turns out, numerical estimates place the Hausdorff dimension of the Lorenz attractor to be approximately 2.0627160! This means that the planes formed by the orbits of the Lorenz attractor have more information than a mere two dimensional surface can provide. This fascinating result was obtained numerically by Viswanath in [8].

This calculation is made by finding initial points which produce periodic orbits in the Lorenz system. Depending on precisely the points chosen, the orbits may alternate between the left and the right wings of the Lorenz system in any combination conceivable before returning to where the orbit started. Specifically, this branching is classified according to the Poincare section, at $z = 27$. These various patterns are referred to as symbol sequences, and are of the form AB, AABB, AAAB, and so on. Because the Lorenz system is chaotic, these periodic cycles must necessarily be repelling, so very precise numerical calculation is necessary. The algorithm described in [8] involves using 100 digit arithmetic for this purpose.

Examining the intersection of these cycles with the Poincare section $z = 27$, the resulting shape takes on the appearance of a Cantor set. The density of points increases as symbol sequences become more complicated. A Cantor set may be thought of as being an infinite binary tree, whose branches directly correspond to the branches in the symbol sequence. This behavior is also discussed extensively in [9]. The distance between starting points of symbol sequences depends in a peculiar manner upon the actual sequences. For two symbol sequences identical in the first $i^{th}$ digits, the distance in their starting points is roughly $0.5^i$. For symbol sequences whose final digits are common, the distance is about a factor of $10^{-5}$ smaller by each symbol at the end. This greatly stresses the significance of how orbits of all periods exist in this chaotic attractor.

In an important formula for discrete systems, given the characteristic multipliers for points in an $m-$cycle, where $F$ is an invertible map of the plane and $F^m(x_i) = x_i$, and $\lambda_i$ is the multiplier at each $x_i$, we may define each $D_m$ as

satisfying the equation:

$$\sum_{i=1}^{m} \lambda_i^{D_m - 1} = 1$$

The limit of $D_m$ is the Hausdorff dimension of the attractor. Such a discrete system may be found by examining the cross sections of the Lorenz cycle. In [8], it is shown that this converges quite quickly to near 2.0627160, and that this is indeed the dimension of the Lorenz attractor.

For other continuous systems, the behavior may not be of this binary variety. The Rossler system, in particular, exhibits a kind of folding which is not analogous to a binary partition. It is however still possible to take a cross section around the main loop and calculate the intersection of the Poincare section with high period cycles and estimate the dimension via the above method. In my research I have not found accurate estimations of this number, but it is presumably just above 2, like the dimension for the Lorenz attractor.

## 5.6 Predictability

While the dynamics in some continuous systems may be very hard to predict, important information may be derived through an investigation of the fractal dimension of the system. This indicates roughly how much area the curve takes up, or rather, how wiggly it is. Generally, the higher the dimension, the harder it is to predict an orbit's eventual behavior.

One of the ways of estimating the dimension of a system is through examining Lyapunov exponents. There are a large number of published methods for determining these numbers, so I shall just mention a few relevant methods. The following is a discussion of the estimation of Lyapunov exponents for continuous systems from Leonov in [5].

If the ODE is $n$-dimensional, the Lyapunov exponent $\nu$ will be an $n$-dimensional vector, describing how perturbations of the initial point will affect long term changes in the attractor, in comparison to exponential divergence. The behavior of Lyapunov exponents is analogous to discrete dynamics. A positive $\nu_1$ implies that the distance between two nearby initial points will diverge, a value near zero implies that there will be little significant variation, and an exponent below zero implies that the orbits between two initial points will converge. Systems may also have both positive and negative Lyapunov exponents. Consider specifically the Lorenz system: along its surface, nearby orbits are very unpredictable, but anything that starts away from the two wings of the butterfly eventually flattens out to meet the surface of the actual attractor. Chaotic systems typically have Lyapunov exponents which are negative, zero, and positive, all at once. When all exponents are negative, the system will produce a an attracting fixed point, when all are negative but one, which is zero, the system will form an attracting cycle. When $m$ are zero and the rest are negative, the system lies on an $m$-dimensional manifold should result.

Let us consider a simple homogenous system:

$$\frac{\mathrm{d}\boldsymbol{x}}{\mathrm{d}t} = \boldsymbol{A}(t)\boldsymbol{x},\ \boldsymbol{x} \in \mathbb{R}^N$$

Again, let $\boldsymbol{X}(t)$ be the fundamental solution for the system, where $\boldsymbol{X}(0) = \boldsymbol{I}$. The square roots of the eigenvalues of matrix $\boldsymbol{X}(t)^*\boldsymbol{X}(t)$ are the singular

numbers of $\boldsymbol{X}(t)$, $\rho_1(t) \geq \rho_2(t) \geq \ldots \geq \rho_n(t)$. The Lyapunov exponents may be defined as:

$$\nu_j = \log \lim_{t \to \infty} \rho_j(t)^{1/t}$$

This is a term that does not lend itself to being calculated directly. Leonov, in [5], describes a very complex way to manipulate eigenvalues and other known constraints on the system to produce precise bounds on each $\nu_j$. When the system is nonlinear, the above technique may be approximated via using a linearization of the system.

# 6 Discrete Dynamical Systems

Without the shelters of continuity or conformality, things can become very complicated indeed. Even if we are only considering two dimensions, infinity ceases to be a point, like it is on the Riemann Sphere. Points may diverge to infinity, but if they go in different directions, their dynamics may be entirely different.

In this last section of this paper, I would like to discuss the application of parameter space to discrete dynamics in broad terms. For convenience sake, the systems we will be concerned with shall be continuously differentiable and parameterized linearly:

$$f_a \in C^1(\mathsf{X} \to \mathsf{X})$$

The function $f_a$ should have a linear dependence on its parameters, ie. $a \mapsto f_a$ is a linear operation. This is a strong condition, as it considerably limits the kinds of parametrical functions we will consider, and disallows behavior such as phase shifting and changing frequencies.

## 6.1 Equivalences and isomorphisms

It is important to show that many functions with apparently different dynamics may in fact represent the same system. This may be illustrated through simple conjugation. A function $f \in \mathsf{X} \to \mathsf{X}$ is conjugate to $g$ if there exists a bijective function $\phi$ such that:

$$f = \phi^{-1} \circ g \circ \phi$$

Thus, we can see inductively that

$$f^{n+1} = f^n \circ f = \phi^{-1} \circ g^n \circ \phi \circ \phi^{-1} \circ g \circ \phi = \phi^{-1} \circ g^{n+1} \circ \phi$$

Symbolic dynamics translates quite well outside of complex analysis, and much insight can be gained from examining the equivalence of conjugations of dynamical systems. In complex analysis, the $2^{nd}$ degree polynomial $az^2 + bz + c$ can be conjugated using möbius transformations to just the case $z^2 + c$. Outside of this case, some parameters in other systems may be found to be unnecessary. Examining the two dimensional quadratic systems that I had originally studied:

$$\begin{aligned} x_{n+1} &= a_1 x_n^2 + a_2 x_n y_n + a_3 y_n^2 + a_4 x_n + a_5 y_n + a_6 \\ y_{n+1} &= b_1 x_n^2 + b_2 x_n y_n + b_3 y_n^2 + b_4 x_n + b_5 y_n + b_6 \end{aligned}$$

It is possible to eliminate several parameters based on equivalence alone. It is also likely that some high dimensional subspaces in the parameter space are equivalent to others based on some elaborate folding transformations.

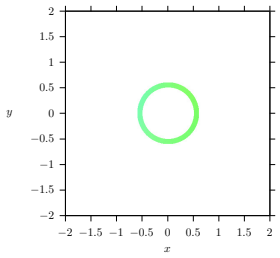


Figure 80: Ring centered on 0 with $r \in [.25, .3]$.

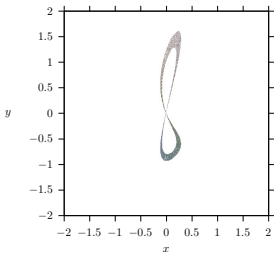


Figure 81: Image of ring under $f$.

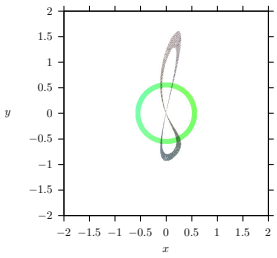


Figure 82: Image overlayed on original ring.

## 6.2 Weakly attracting fixed points

The concept of weakly attracting fixed points seems rather surprising, since in complex analysis, the distinction between attracting, neutral, and repelling is very straightforward. With multiple dimensions, fixed points can become very unpredictable. Strongly attracting fixed points in general dynamical systems most closely resemble the attracting fixed points in complex analysis. However, even if all the absolute values of the eigenvalues of the function's derivative are less than one, at some fixed point, the norm of the Jacobian matrix may still be greater than one. This means that points near the fixed points may be drawn in along the correct axis, but the function is still not a contraction in any ball around the fixed point. Consider the following map:

$$f(x, y) = \begin{pmatrix} x^2 + 2xy \\ 2x - 2x^2 - 2xy \end{pmatrix}$$

There are fixed points in this map at $(0, 0)$ and $(1, 0)$, and the eigenvalues of the derivative at both points are both zero. If one follows the orbits of points near each of these fixed points, one can see that the orbits eventually fall into the nearest fixed point. However, the norms of the derivatives at the fixed points are greater than one, regardless of norm chosen. Examining closely the point $(0, 0)$, we can see that any point on the diagonal line $y = x$ is first pushed away from $(0, 0)$, but then drawn back in. This means that there is still no ball in which the function is a contraction mapping, but there is a ball in which all points are guaranteed to be drawn in. In this respect these weakly attracting fixed points behave similarly to neutral fixed points in the complex analysis sense.

The following images display a ring around the point $(0, 0)$ and its image under the mapping. The projection exhibits a very peculiar twisting behavior, and it is possible to see how some points chosen near the fixed point will always be pushed away. However, there is also a transformation that spins the ring around, so points that are pushed away will always rotate to one of the angles at which they are pulled back in.

## 6.3 What it means to be chaotic

As in continuous systems, chaos can originate from orbits becoming drawn towards multiple fixed points or cycles, and alternating between them. Chaos can result from some irrational folding of the phase space into itself. Orbits

under some rational map $R$ in $\mathbb{C}$ generally will be drawn into some sort of periodic structure, save for points chosen on the Julia set. The Julia set in a complex map is a fixed component, invariant under $R$, and also having the property that any two distinct points chosen in the Julia set, no matter how close together, will eventually be separated. It is in this way that Julia sets are chaotic structures under rational maps. In the complex sense, orbits exhibit chaotic behavior in relatively rare situations, as Julia sets are fairly narrow. In both continuous and discrete systems, orbits may be chaotic in a much broader range of circumstances. Chaos is actually surprisingly common in both types of systems.

One of the defining factors in chaotic systems is the role of repelling cycles. Often chaotic dynamics are formed by the existence of a couple of stable or somewhat stable fixed points or cycles, and the chaotic behavior arises from points interacting with both cycles. However, when this is the case, multitudes of cycles manage to become balanced in between the two cycles, and these precarious bands tend to be neutral or repelling cycles. These cycles are, in fact, dense in chaotic systems. Interestingly, in chaotic systems there are necessarily repelling cycles of *all* periods. Recall that the Julia set is the closure of both repelling cycles and chaotic orbits. It has been established several times (via Sarkovskii's theorem as well as the well known paper by Yorke and Li [23]), that a necessary feature for chaos to exist is for the given system to have a cycle of period three.

## 6.4 Stability and Lyapunov exponents

Lyapunov exponents are a tool for measuring the stability in a system. They tend to be an invaluable tool for the purposes of this measurement, however they are often used or defined in different ways. At the end of the day, each use or definition seems to be getting after the same general concept, but it is of crucial importance to clarify how the exponent is used in this paper and what definitions and approximations we use to obtain it.

When all of the Lyapunov exponents are negative, there tend to be attracting fixed points or cycles. When one of the exponents is zero, there tends to be some kind of neutral plane which neither attracts nor repels. If one exponent is zero and the rest are zero or negative, then there will be an attraction towards something like a limit cycle, as the one plane is neutral and permits movement, but the other exponents draw in nearby points. Positive exponents inject some form of chaotic behavior. If there is one positive exponent and the rest are negative, there is likely to be some kind of limit cycle, along which the movement is unpredictable. For instance, there could be an angle doubling map.

The balance of these can form quite interesting structures, especially in working with more than two dimensions. When I had been investigating strange attractors in three dimensions, I ran across attractors which appeared to be just loops of points in three dimensional space. Since those attractors had been picked up by my program as having a positive Lyapunov exponent, it would be likely that chaotic behavior was taking place on that loop, probably in the form of an angle doubling map of sorts. Other times, my program would find attractors which seemed to be like two dimensional manifolds in three dimensional space. It seemed clear that what was occurring as the loops transformed into the planes was that $\nu_2$ was changing sign from negative to positive. Thus

as the degree of instability along that dimension increased, the system came to express more information than just that of a one dimensional manifold in space. Bearing this in mind, it should come as no surprise that Lyapunov exponents are also useful tools to also measure the dimension of an attractor. Unfortunately, a detailed analysis of how this is done is outside of the scope of this paper.

Previously, we had seen a little discussion of Leonov's bounds of Lyapunov exponents for the continuous case. He also provides a thorough analysis of the discrete case as well. We shall begin by observing a simple linear system and comparing its asymptotic properties to more useful cases. Consider the following simple system:

$$\boldsymbol{x}_{k+1} = A(k)\boldsymbol{x}_k$$

This system will have a fundamental matrix $X(k)$, such that $\boldsymbol{x}_k = X(k)\boldsymbol{x}_0$:

$$X(k) = \prod_{j=0}^{k} A(j)$$

Recall this kind of construction from the previous discussion of continuous systems.

The Lyapunov exponents $\nu_j$ in the discrete case are defined as:

$$\nu_j = \log \lim_{k\to\infty} \rho_j(k)^{1/k}$$

Where $\rho_j$ are the square roots of the eigenvalues of $X(k)^*X(k)$.

It is possible to obtain a variety of bounds on each $\rho_j$ by finding quadratic forms such that the application of the forms on each $A(k)$ satisfies several elaborate inequalities. The general procedure starts with finding a symmetric matrix $H$ with no less than $m$ positive (or negative) eigenvalues. The sign of the number of eigenvalues will determine whether $H$ will constrain either $\rho_{N-m+1}$ or $\rho_m$ from above or below, respectively. $H$ will define a quadratic form $V(\boldsymbol{x}) = \boldsymbol{x}^*H\boldsymbol{x}$. Then suppose $\exists\lambda > 0$, and $\boldsymbol{z} \in \Omega$ where $\Omega$ is either $\{\boldsymbol{x} \in \mathbb{R}^N \mid V(\boldsymbol{x}) < 0\}$ or $\mathbb{R}^N$, depending on whether we are looking for a lower or upper bound, respectively. Suppose that:

$$\frac{1}{\lambda^2}V(A(k)\boldsymbol{z}) \leq V(\boldsymbol{z}).$$

Then $\exists\beta > 0$ such that $\rho_m(k) \geq \beta\lambda^k$, $\forall k \in \mathbb{N}^\times$. Note that this final bound does not depend directly on $H$ or $\boldsymbol{z}$, but as long as they exist, this bound may be asserted. Conversely, if $\forall k \in \mathbb{N}^\times$, $\det A(k) \neq 0$ then:

$$\frac{1}{\lambda^2}V(A(k)^*\boldsymbol{z}) \leq V(\boldsymbol{z}).$$

implies that $\gamma$ such that $\rho_{n-m+1}(k) \leq \gamma\lambda^k$, $\forall k \in \mathbb{N}^\times$. Therefore we may find both upper and lower bounds on each $\rho_j$. The advantage of this approach is that it is possible to continue to find better values of $\lambda$ such that one can produce tighter and tighter bounds. From the very beginning we can see that there is a dual nature to this procedure. Leonov continues this method, but it involves more intricate nuances in the different qualities of the upper and lower bounds. Regardless, the above results are enough to derive some simple bounds on each $\nu_j$. Because $\nu_j$ is defined as the limit of an exponent, and $\rho_j(k) \geq \beta\lambda^k$, then:

$$\nu_j = \log \lim_{k\to\infty} \rho(k)^{1/k} \geq \log \lim_{k\to\infty} \beta^{1/k}\lambda = \log\lambda$$

Leonov continues to produce Hermitian forms that make use of these constraints in order to place bounds on the Hausdorff dimension of the attractor. I shall not follow through his argument, but it is an example of one of the ways in which analysis of Lyapunov exponents may reveal volumes regarding the dynamics of the system.

From a computational perspective, it is also useful to estimate Lyapunov exponents not as a vector, but as a single term. When this is the case, the single term, $\nu$, is $\nu_1$, the largest Lyapunov exponent. It is important to see how it is calculated though, as it would be almost impossible to fit the previous analysis into a simple computer program. One way of estimating this, is to choose random points near the initial point of the orbit under consideration, and compare their divergence from the orbit, though it is important to note that this method is only appropriate for approximations. After each application of the function, they would be scaled back towards a uniform distance from the next iterate of the point. This was the method originally used in Paul Bourke's page for creating strange attractors [20].

$$\nu \approx \lim_{n\to\infty} \frac{1}{n} \sum_{i=0}^{n} \log \frac{\|f(\boldsymbol{x}_i + \delta \boldsymbol{v}_i) - f(\boldsymbol{x}_i)\|}{\delta}$$

Typically, $\boldsymbol{v}_0$ would initially be a randomly chosen unit vector, but

$$\boldsymbol{v}_i = \frac{f(\boldsymbol{x}_i + \delta \boldsymbol{v}_i) - f(\boldsymbol{x}_i)}{\|f(\boldsymbol{x}_i + \delta \boldsymbol{v}_i) - f(\boldsymbol{x}_i)\|}$$

where $\delta$ would be small. Examining this approach, the natural thing to do is to take the limit as $\delta \to 0$, and we find that the term under the logarithm is:

$$\lim_{\delta\to 0} \frac{\|f(\boldsymbol{x}_i + \delta \boldsymbol{v}_i) - f(\boldsymbol{x}_i)\|}{\delta} = \|f'(\boldsymbol{x}_i)\boldsymbol{v}_i\|$$

It is easy to suspect that the term is only $\|f'(\boldsymbol{x}_i)\|$; however, through numerical experiments, this would not seem to be the case. If we actually choose random points offset from $\boldsymbol{x}_i$ each iteration, we will approximate the actual exponent. So what appears to be taking place here is some dependence on the nonlinear properties of $f$, since its derivative is not enough to do the job.

## 6.5 Analogy to Complex Analysis

While things become progressively more complicated by taking away conformality and adding dimensions, it is still possible to make analogies to complex analysis. It is possible to describe basins of attraction for dynamical systems, and therefore it should be possible to describe what happens to these basins as parameters are varied. (Unfortunately, these are much more difficult to measure as there is not a clear way to find this basin without testing a lot of points.)

Ben Bielefeld, et al. [24] studied the nonholomorphic family of functions $f_\alpha \in \mathbb{C} \to \mathbb{C}$, $f = z \mapsto |z|^{2\alpha-2}z^2 + c$. This case was also studied by Szczyrek [11] as well as by Bruin and Van Noort [15]. While it is nonconformal, it still persists in being quasiconformal, so it is not tremendously estranged from Complex Analysis. It is observed that while certain properties familiar to holomorphic functions do break down, others are able to be maintained. Concepts such as the Mandelbrot and Julia sets still remain intact, though the Julia sets become

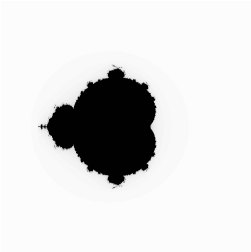

Figure 83: Mandelbrot set with $\alpha = 1.5$.

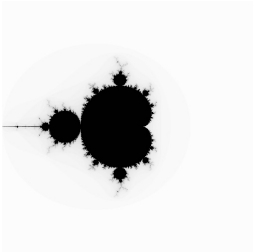

Figure 84: Mandelbrot set with $\alpha = 1.0$.

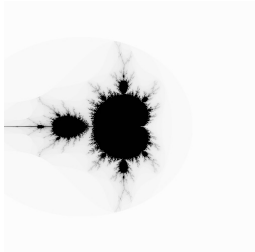

Figure 85: Mandelbrot set with $\alpha = 0.8$.

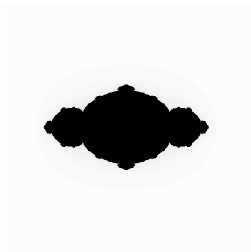

Figure 86: Julia set at $c = -1$ with $\alpha = 1.5$.

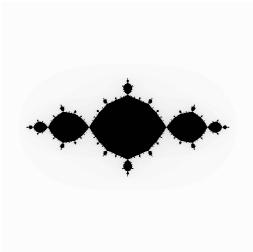

Figure 87: Julia set at $c = -1$ with $\alpha = 1.0$.

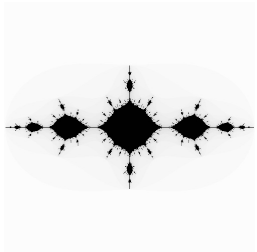

Figure 88: Julia set at $c = -1$ with $\alpha = 0.8$.

smooth for some $\alpha > 1$. The Julia sets remain connected, so it is still possible to analyze external rays. However, certain things become totally lost outside the nonconformal setting. For instance, periodic attractors do not necessarily attract the critical point, which overturns the method by which the Mandelbrot set is most often computationally determined. Some images of Mandelbrot and Julia sets under these mappings are presented on the following page.

Looking further beyond the scope of complex analysis, many more complications can arise. Julia-like sets do not necessarily need to be connected, and in more than one dimension, often critical points cease to exist entirely. Nonetheless, when functions are parameterized and perturbed only slightly, periodic orbits and their basins of attraction tend to continue to exist and be perturbed as well. The invariant sets that are produced by strange attractors are necessarily compact, and thus they should have borders as well. These fractal borders are what most closely resemble Julia sets in complex analysis. In [6], it is shown that when multiple stable cycles exist, there may be entangled boundaries with definite fractal properties. It would make sense for there to be some kind of Mandelbrot-like set in parameter space which abstractly governs the dynamics of all of these attractors.

# 7 Conclusion

In this paper, we have discussed a multitude of dynamical systems, and addressed the relevance of parameter space in each of them. We have seen how the smooth behavior of continuous systems is affected by perturbations in parameters, and seen how strange attractors may emerge in such systems. Addi-

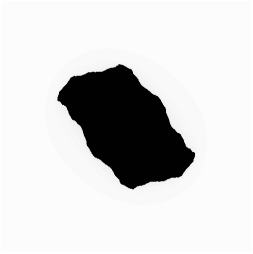

Figure 89: Julia set at $c = -0.1264 + 0.6496i$ with $\alpha = 1.5$.

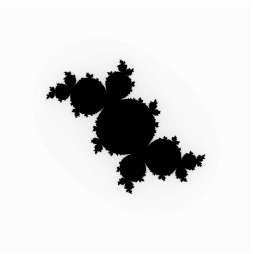

Figure 90: Julia set at $c = -0.1264 + 0.6496i$ with $\alpha = 1.0$.

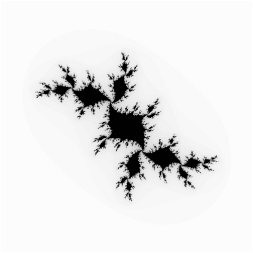

Figure 91: Julia set at $c = -0.1264 + 0.6496i$ with $\alpha = 0.8$.

tionally, we have seen the complex case, in which dynamics are controlled by intricate combinatorial patterns that can be described symbolically. The most famed example of parameter space in complex analysis is the Mandelbrot set, which describes both the structure of Julia sets, and the behavior of the orbits of 0. Even though the complex plane holds a great range of dynamics, it behaves in a fundamentally one dimensional manner under conformal mappings. When this conformality is removed, as we have seen in the case of the Hénon map, there also exists a parameter space that may be represented in a manner as to describe the dynamics under those parameters. We have seen several portions of the Hénon parameter map, and the correlation of the structure of those regions with the structure of the Julia-like sets.

Overall, parameter space can tell us a great deal about the behavior of a dynamical system. Particularly, it can show us where regions are that express different kinds of long-term behavior. Examining these maps often can lead to discovery of surprising bits of unexpected behavior. The density of stable sections in the chaotic region of the Hénon parameter map is particularly surprising, as it is analogous to how repelling periodic cycles are dense in chaotic systems. This suggests that if we have parametric control over a system and it is in one of these chaotic regions, we could coax just about any stable periodic cycle out of the system by a very slight perturbation of parameters. The usefulness of chaos in systems has been well discussed in "Controlling Chaos" [4], which discusses in detail the applications of this technique to real world situations.

In this paper we have illustrated the Hénon parameter map via using colors to show periods and Lyapunov exponents. The images used were produced by carefully sampling initial points and taking averages over those points that did not diverge. It would be worthwhile in future research to examine carefully what points are necessary to choose in order to obtain accurate estimations of these values. Furthermore, this would drastically reduce the computation cost for mapping out the features of the parameter space. There are many other mysterious regions in the Hénon parameter map, specifically, and it would be worthwhile to see precisely what is taking place in these regions. Specifically, I would very much like to see what dynamics are causing the stable sections to jump out to the areas that diverge to infinity. Many fascinating structures and behavior have become visible by observing the Hénon map from a parametrical perspective, and it would prove fruitful to see how this analysis plays out in

other dynamical systems, to observe what discoveries could be made in those domains.

# A Source Code

## A.1 Common Files

These files are concerned with loading and saving images. These files can produce Windows Bitmap images. This is how I produced most of the graphics that are included in this paper. The function "WriteBMP(filename)" saves a bitmap of what is included in the two dimensional array "view". This is plotted such that the coordinates resemble those commonly used in mathematics, where "view[0][0]" is the bottom leftmost pixel, (containing the smallest value in both $x$ and $y$ axes), and "view[RES-1][RES-1]" is the top rightmost pixel, (containing the largest value in both axes). This is done to ensure that the images are not flipped when presented in the axes in this paper.

### A.1.1 base.h

```
#ifndef BASE_H
#define BASE_H


#include <math.h>

struct color
{
    double R,G,B;
    color() : R(0), G(0), B(0) {}
    inline color(double r, double g, double b) : R(r), G(g), B(b) {}
    void flatten()
    {
        if(R<0) R=0;
        else if(R>1) R=1;
        if(G<0) G=0;
        else if(G>1) G=1;
        if(B<0) B=0;
        else if(B>1) B=1;
    }
};


#define RES 2000

extern color view[RES][RES];

#endif
```

### A.1.2 base.cpp

```
#include "base.h"

color view[RES][RES];
```

### A.1.3 bitmap.h

```
#ifndef BITMAP_H
#define BITMAP_H

void WriteBMP(char filename[]);

#endif
```

### A.1.4 bitmap.cpp

```
#include <fstream>

#include "bitmap.h"
#include "base.h"

using namespace std;

void writeDWORD(ofstream &Out,unsigned int d);
void writeWORD(ofstream &Out,unsigned int d);
void writeCHAR(ofstream &Out,unsigned int d);

void WriteBMP(char filename[])
{
    ofstream Out;
    Out.open(filename,ios::binary);
    if(Out.fail())
        return;

    Out << "BM";    //Windows Bitmap ID
    writeDWORD(Out,36+3*RES*RES);   //Filesize
    writeDWORD(Out,0);  //some stupid thing
    writeDWORD(Out,0x36);   //offset of bitmap data
    writeDWORD(Out,0x28); //windows standard info header size
    writeDWORD(Out,RES); //width of bitmap
    writeDWORD(Out,RES); //height of bitmap
    writeWORD(Out,1); // "planes" in bitmap
    writeWORD(Out,24); // image depth in bitmap
    writeDWORD(Out,0); // compression
    writeDWORD(Out,0); // something about data size...
    writeDWORD(Out,2834); // XResoultion...
    writeDWORD(Out,2834); // YResolution
    writeDWORD(Out,0); //colors (0 because 24bit)
    writeDWORD(Out,0); //important colors

    // forward reading of the y coordinate should produce
    // the image being upside-down, however, the Windows BMP
```

```
    // file format encodes the y coordinate upside-down anyway
    // so the correct orientation is preserved.
    for(int y=0;y<RES;y++)
    for(int x=0;x<RES;x++)
    {
        writeCHAR(Out,int(view[x][y].B*255));
        writeCHAR(Out,int(view[x][y].G*255));
        writeCHAR(Out,int(view[x][y].R*255));
    }
}

void writeDWORD(ofstream &Out,unsigned int d)
{
    writeWORD(Out,d%65536);
    writeWORD(Out,d/65536);
}

void writeWORD(ofstream &Out,unsigned int d)
{
    Out << char(d%256);
    Out << char(d/256);
}

void writeCHAR(ofstream &Out,unsigned int d)
{
    Out << char(d);
}
```

## A.2 Attraction Test

This program produces images that display the projection of a region in the plane under iterations of a quadratic map, through either illustration of the projected region, or through color.

### A.2.1 main.cpp

```
#include <stdlib.h>
#include <math.h>
#include <iostream>
#include <fstream>
#include <time.h>
#include <vector>

using namespace std;

#include "bitmap.h"
#include "base.h"

double drand() //returns a double between -1 and 1
{
    return (double(rand())/RAND_MAX-.5)*2;
}
```

```
double squash(double x)
{
    return (1+x/(fabs(x)+1))/2;
}

#define ITERSIZE 1000
#define LYAPUNOVAT 100
#define max(a,b) (a<b ? b : a)
#define min(a,b) (a<b ? a : b)
#define ABS(x) (x<0 ? -x : x)


void main()
{
    int i,X,Y;

    for(X=0;X<RES;X++)
    {
    cout << X << endl;
    for(Y=0;Y<RES;Y++)
    {

        double x,y,x1,y1,x0,y0;
        x0 = x = ((double)X/RES) * 4 - 2;
        y0 = y = ((double)Y/RES) * 4 - 2;

        double xr,yr;
        //xr = x0 - -0.4541344013;
        //yr = y0 - 0.1844711485;
        xr = x0 - -0.0104387891;
        yr = y0 - 0.2096393646;

        xr = xr*xr;
        yr = yr*yr;

        // this will only use points which are between
        // .1 and .2 units from the origin.
        if(sqrt(xr + yr)>.1)// || sqrt(xr + yr)<.2)
            continue;

        double a1,a2,a3,a4,a5,a6;
        double b1,b2,b3,b4,b5,b6;

        a1 = -0.4252449110;
        a2 = 0.4798120060;
        a3 = -0.4645527512;
        a4 = -0.7605822932;
        a5 = 0.5426801355;
        a6 = -0.7559434797;

        b1 = -1.2936796167;
        b2 = -0.7068697165;
        b3 = -0.4903103732;
```

```
        b4 = 1.8258003479;
        b5 = -0.4433118686;
        b6 = 1.3196813868;

        // this is the number of iterations that the function is applied
        for(i=0;i<5;i++)
        {
            x1 = a1*x*x + a2*x*y + a3*y*y + a4*x + a5*y + a6;
            y1 = b1*x*x + b2*x*y + b3*y*y + b4*x + b5*y + b6;

            x = x1;
            y = y1;
        }

        // this option is used to draw the destination of the iterated point
        // the value of the point is represented as a color. Mid tones represent
        // values towards zero, bright or dark colors represent colors that tend
        // towards infinity in one direction or another.
    //  view[X][Y] = color(squash(x),0,squash(y));

        // this option displays the inverse of the above: a point is given the color
        // of where it was initially located, and placed where it wound up after
        // being iterated under the function.
        if((x/4+.5) >= 0 && (x/4+.5) < 1 && (y/4+.5) >= 0 && (y/4+.5) < 1)
            view[(int)((x/4+.5)*RES)][(int)((y/4+.5)*RES)] = color(x0/4+.5,.5,y0/4+.5);
    }
    }
    WriteBMP("out.bmp");
}
```

## A.3 Cycle Test

This program attempts to find multiple attracting cycles. It samples random points in parameter space, tests for attracting periodic structures, and samples again to find separate attracting periodic structures. This program does discard multiple seemingly attracting cycles when there is chaos. This decision was made due to a drastic number of false positives.

### A.3.1 main.cpp

```
#include <stdio.h>
#include <stdlib.h>
#include <time.h>
#include <math.h>

double a[6];
double b[6];

#define max(a,b) ((a)>(b) ? (a) : (b))
#define abs(a) ((a)>0 ? (a) : -(a))

#define MAXPERIOD       100
```

```
#define PERIODCONF      10
#define MAXITERATIONS       10000
#define LYAPUNOVAT      1000
#define PI          3.14159265358979323846264338327795
#define EPSILON         .01
#define TESTEPSILON     .0001
#define LEFTMOSTEPSILON     .1
#define OUTOFBOUNDS     100
#define TESTS           1000000

double drand(double range)
{
    return 2*range*((double)rand())/RAND_MAX-range;
}

void randomize_params(double range)
{
    for(int i=0;i<6;i++)
    {
        a[i] = drand(range);
        b[i] = drand(range);
    }
}

void f(double x, double y, double *x1, double *y1)
{
    *x1 = a[0]*x*x + a[1]*x*y + a[2]*y*y + a[3]*x + a[4]*y + a[5];
    *y1 = b[0]*x*x + b[1]*x*y + b[2]*y*y + b[3]*x + b[4]*y + b[5];
}

void fprime(double x, double y, double *A)
{
    A[0] = a[3] + 2*x*a[0] + y*a[1]; // dx1/dx
    A[1] = a[4] + x*a[1] + 2*y*a[2]; // dx1/dy
    A[2] = a[3] + 2*x*b[0] + y*b[1]; // dy1/dx
    A[3] = a[4] + x*b[1] + 2*y*b[2]; // dy1/dy
}

void near_point(double x, double y, double epsilon, double *x1, double *y1)
{
    // using L2 norm
    double theta = drand(PI);
    *x1 = x + epsilon*cos(theta);
    *y1 = y + epsilon*sin(theta);
}

double matrix_norm(double *A)
{
    // using derived L2 norm
    return sqrt(A[0]*A[0] + A[1]*A[1] + A[2]*A[2] + A[3]*A[3]);
}

double vector_norm(double x, double y)
{
```

```
    // using L2 norm
    return sqrt(x*x+y*y);
}

void matrix_mult(double *A, double *B, double *C)
{
    C[0] = A[0]*B[0] + A[1]*B[2];
    C[1] = A[0]*B[1] + A[1]*B[3];
    C[2] = A[2]*B[0] + A[3]*B[2];
    C[3] = A[2]*B[1] + A[3]*B[3];
}


bool test_cycle(double x0, double y0, int *period,
    double *lyap, double *lmostx, double *lmosty)
{
    int i,j;

    double x=x0 ,y=y0;
    double x1,y1, x2,y2;

    bool periodic = false;
    double lyapunov=0;

    double logepsilon = log(EPSILON);

    for(i=0;i<MAXITERATIONS;i++)
    {
        f(x,y, &x1,&y1);

        if(i>LYAPUNOVAT)
        {
            double xe,ye, xe1,ye1;
            near_point(x,y,EPSILON,&xe,&ye);

            f(xe,ye, &xe1,&ye1);
            lyapunov += log(vector_norm(x1-xe1,y1-ye1)) - logepsilon;
        }

        x = x1; y = y1;
        if(vector_norm(x,y) > OUTOFBOUNDS)
            return false;
    }

    lyapunov = lyapunov/(MAXITERATIONS-LYAPUNOVAT);
    *lyap = lyapunov;

    // x2 and y2 are the last point on the orbit
    // if the system is periodic, then this step will catch the period

    x2 = x; y2 = y;

    *lmostx = x;
    *lmosty = y;
```

```
if(lyapunov<0)
for(j=0;j<PERIODCONF;j++)
{
    for(i=0;i<MAXPERIOD;i++)
    {
        f(x,y, &x1,&y1);

        if(*lmostx < x1)
        {
            // catch the leftmost point
            *lmostx = x1;
            *lmosty = y1;
        }

        x = x1; y = y1;

        if(j!=0)
        {
            if(*period == i+1)
                if(vector_norm(x-x2,y-y2) < TESTEPSILON)
                    continue;
                else
                {
                    periodic = false;
                    break;
                }
        }
        else
            if(vector_norm(x-x2,y-y2) < TESTEPSILON)
            {
                periodic = true;
                *period = i+1;

                break;
            }

        if(vector_norm(x,y) > OUTOFBOUNDS)
            return false;
    }

    if(!periodic)
        break;
}

if(!periodic) // system is chaotic then
{
    *period = 0;

    for(i=0;i<MAXITERATIONS;i++)
    {
        if(*lmostx < x1)
        {
            // catch the leftmost point
```

```
                *lmostx = x1;
                *lmosty = y1;
            }

            f(x,y, &x1,&y1);

            x = x1; y = y1;
            if(vector_norm(x,y) > OUTOFBOUNDS)
                return false;
        }
    }

    return true;
}

double get_derivative_norm(double x, double y, int period)
{
    int i,j;

    double x1,y1;
    double A[4],B[4],C[4];

    B[0] = 1;
    B[1] = 0;
    B[2] = 0;
    B[3] = 1;

    for(i=0;i<period;i++)
    {
        f(x,y, &x1,&y1);

        fprime(x,y,A);
        matrix_mult(A,B,C);

        for(j=0;j<4;j++)
            B[j] = C[j];

        x = x1; y = y1;
        if(vector_norm(x,y) > OUTOFBOUNDS)
            return false;
    }

    return matrix_norm(B);
}

int main()
{
    srand(time(0));

    int stable_structures = 0;
    int chaotic_structures = 0;
    int nonattracting_periods = 0;
    int questionable_periods = 0;
    int valid_periods = 0;
```

```
int two_structures = 0;
int period_and_chaos = 0;
int period_and_period = 0;

int i,j,k;
for(i=0;i<TESTS;i++)
{
    printf("\ntest# %d\n",i+1);

    randomize_params(2);

    int period, period1;
    double lyap, lmostx, lmosty;
    double lyap1, lmostx1, lmosty1;

    double x0,y0;
    double x1,y1;

    bool good = false;
    for(j=0;j<100;j++)
    {
        x0 = drand(2);
        y0 = drand(2);
        if(test_cycle(x0,y0, &period, &lyap, &lmostx, &lmosty))
            good = true;
    }

    if(!good)
        continue;

    stable_structures++;
    printf("Found stable structure!\n");
    printf("parameters:\n");

    printf("%.10f %.10f %.10f\n", a[0], a[1], a[2]);
    printf("%.10f %.10f %.10f\n", a[3], a[4], a[5]);
    printf("%.10f %.10f %.10f\n", b[0], b[1], b[2]);
    printf("%.10f %.10f %.10f\n", b[3], b[4], b[5]);

    printf("leftmost x:%.10f y:%.10f\n",lmostx,lmosty);
    printf("lyapunov: %.10f\n",lyap);
    if(period==0)
    {
        printf("Structure is chaotic.\n");
        chaotic_structures++;
        continue;
    }
    else
    {
        printf("Structure is periodic with period: %d.\n",period);

        double dnorm = get_derivative_norm(lmostx,lmosty,period);
        printf("Has derivative norm: %f\n",dnorm);
```

```
    if(dnorm > 1)
    {
        printf("Not technically attracting\n");
        nonattracting_periods++;
        continue;
    }

    if(dnorm < .000001)
    {
        printf("Not sure this is valid...\n");
        questionable_periods++;
        continue;
    }

    valid_periods++;
}

// here we have a stable structure somewhere
// let's try to find another one.

bool good1 = false;
for(k=0;k<20 && !good1;k++)
{
    printf(".");
    good = false;
    for(j=0;j<100;j++)
    {
        x1 = drand(2);
        y1 = drand(2);
        if(test_cycle(x1,y1, &period1, &lyap1, &lmostx1, &lmosty1))
            good = true;
    }
    if(vector_norm(lmostx1-lmostx,lmosty1-lmosty)>LEFTMOSTEPSILON)
        good1 = true;
}
printf("\n");
if(!good1)
    continue;

two_structures++;
printf("Found separate structure:\n");
printf("leftmost x:%.10f y:%.10f\n",lmostx1,lmosty1);
printf("lyapunov: %.10f\n",lyap1);

double dnorm = 2;

if(period1==0)
{
    period_and_chaos++;
    printf("Structure is chaotic.\n");
}
else
{
    period_and_period++;
```

```
            printf("Structure is periodic with period: %d.\n",period1);

            dnorm = get_derivative_norm(lmostx1,lmosty1,period1);

            if(dnorm < .000001)
            {
                printf("Not sure this is valid...\n");
                continue;
            }

            printf("Has derivative norm: %f\n",dnorm);
        }

        if(period==1 && period1==1)
            printf("This is probably invalid\n");
        else if(dnorm < 1)
            break;
        else continue;
    }

    printf("\n ***END***\n\n");
    printf("The rundown:\n");
    printf("Stable Structures:      %d\n",stable_structures);
    printf("Chaotic structures:     %d\n",chaotic_structures);
    printf("Nonattracting periodic: %d\n",nonattracting_periods);
    printf("Questionable periodic:  %d\n",questionable_periods);
    printf("Valid periodic:         %d\n",valid_periods);
    printf("Two Structures:         %d\n",two_structures);
    printf("Period and Chaos:       %d\n",period_and_chaos);
    printf("Period and Period:      %d\n",period_and_period);

    getchar();
    return 0;
}
```

## A.4 Hénon Map

These programs display both the parameter space and the phase space under the Hénon map. The file "attractormap.cpp" plots the parameter space, samples heuristically to locate non-diverging orbits, and colors the regions accordingly. Filled-in Julia-like sets and prominent orbits are plotted using "henon julia.cpp". This program colors regions according to the ultimate destination of the points in the phase space.

### A.4.1 dyn.h

```
#ifndef DYN_H
#define DYN_H

#include <stdlib.h>
#include <math.h>

#define pi 3.14159265358979323846264338327795
```

```
#define PERIODTEST 5

double drand();
double squash(double x);

struct parameter_set
{
    double a;
    double b;
    parameter_set(double _a, double _b) : a(_a), b(_b) {}
    parameter_set() : a(0), b(0) {}
};
parameter_set operator+(parameter_set a, parameter_set b);
parameter_set operator*(double c, parameter_set a);
parameter_set randparam();

struct point
{
    double x;
    double y;
    point(double _x, double _y) : x(_x), y(_y) {}
    point() : x(0), y(0) {}
};
inline point operator+(point a, point b);
inline point operator-(point a, point b);
point operator*(double c, point a);

double norml1(point a);
double norml2(point a);
double dist(point a, point b);
point randpoint();


typedef point (*dynmap)(parameter_set*, point);

void analyze(parameter_set a, dynmap f, point x0, int *period, double *lyapunov);

#endif
```

### A.4.2 dyn.cpp

```
#include "dyn.h"
#include <vector>

using namespace std;


#define ITERSIZE 20000
#define LYAPUNOVAT 5000
#define epsilon 1e-5
```

```
double drand() // returns a double between -1 and 1
{
    return (double(rand())/RAND_MAX-.5)*2;
}

double squash(double x) // compresses a value between -1 and 1
{
    return (1+x/(fabs(x)+1))/2;
}

parameter_set operator+(parameter_set a, parameter_set b)
{
    return parameter_set(a.a+b.a,a.b+b.b);
}

parameter_set operator*(double c, parameter_set a)
{
    return parameter_set(c*a.a,c*a.b);
}

parameter_set randparam()
{
    return parameter_set(cos(pi*drand()),sin(pi*drand()));
}

inline point operator+(point a, point b) {return point(a.x+b.x,a.y+b.y);}
inline point operator-(point a, point b) {return point(a.x-b.x,a.y-b.y);}
point operator*(double c, point a) {return point(c*a.x,c*a.y);}

double norml1(point a) {return fabs(a.x)+fabs(a.y);}
double norml2(point a) {return sqrt(a.x*a.x+a.y*a.y);}
double dist(point a, point b) {return norml2(a-b);}
point randpoint() {return point(cos(pi*drand()),sin(pi*drand()));}


static vector<point> x(ITERSIZE);


/* analyze
 * analyze takes a parameter, a mapping, and an initial point, and determines
 * the period and the lyapunov exponent of the resulting sequence.
 *
 * If the sequence is divergent, lyapunov is set to zero,
 * and period is set to -1. If the sequence is periodic, the
 * iteration breaks, the lyapunov exponent is calculated, and
 * the period is recorded. Otherwise, the sequence is nonperiodic.
 * In which case, the period is set to zero, and the lyapunov
 * is recorded.
 */
void analyze(parameter_set a, dynmap f, point x0, int *period, double *lyapunov)
{
    double logepsilon = log(epsilon);

    bool good=true;
```

```
x[0]=x0;
int period0 = 0;
double lyapunov0 = 0;

int i,j;
point xi, xiprev=x0;
for(i=1; i<ITERSIZE && good; i++)
{
    x[i] = xi = f(&a, xiprev);

    if(norml1(xi) > 1e5)
    {
        good=false;
        period0=-1;
    }

    if(i>2*PERIODTEST)
    for(j=1;j<PERIODTEST && good;j++)
        if(norml1(xi-x[i-j])<1e-15 && norml1(xi-x[i-2*j])<1e-15)
        {
            if(norml1(xi-x[i-j])==0)
                period0=1;
            else
                period0=j;
            good=false;
        }

    if(i>LYAPUNOVAT)
    {
        point xe = epsilon*randpoint() + xiprev;
        xe = f(&a,xe);
        lyapunov0 += log(dist(xe,xi)) - logepsilon;
    }

    xiprev=xi;
}

if(!good && period0==-1)
{
    // divergent
    *period=-1;
    *lyapunov=0;
}
else if(!good && period0>0)
{
    // need to recalculate lyapunov with limit period points.
    lyapunov0=0;
    for(j=0;j<period0;j++)
    {
        point xe = epsilon*randpoint() + x[i-1-j];
        xe = f(&a,xe);
        lyapunov0 += log(dist(xe,x[i-j])) - logepsilon;
    }
```

```
        *period = period0;
        *lyapunov = lyapunov0/period0;
    }
    else // otherwise good, period0 must be zero
    {
        *period = 0;
        *lyapunov = lyapunov0/(ITERSIZE-LYAPUNOVAT);
    }
}
```

### A.4.3 attractormap.cpp

```
// generates a grid of attractors and saves a bitmap "out.bmp"
// representing which ones elicit what behavior.

#include <stdlib.h>
#include <math.h>
#include <iostream>
#include <fstream>
#include <time.h>
#include <vector>

using namespace std;

#include "bitmap.h"
#include "base.h"
#include "dyn.h"


#define INITIALTESTS 5

point f(parameter_set* a, point x)
{
    return point( a->a - x.x*x.x + a->b*x.y , x.x );
}

int __cdecl main()
{
    srand((unsigned)time(0));

    int k,X,Y;

    double lyapunov[INITIALTESTS];
    int period[INITIALTESTS];

    double lyapunov1[INITIALTESTS];
    int period1[INITIALTESTS];
    // period is 0 if nonconvergent
    // -1 if goes to infinity
    // a positive integer if any other period
```

```
double resolution = 4.0;
double xcenter = 0.0;
double ycenter = 0.0;

for(X=0;X<RES;X++)
{
cout << X << endl;
for(Y=0;Y<RES;Y++)
{
    parameter_set a(-(resolution*X)/RES+.5*resolution+xcenter,
            -(resolution*Y)/RES+.5*resolution+ycenter);

    analyze(a,f,fprime,point(0,0),&period[0],&lyapunov[0]);
    for(k=1;k<5;k++)
    {
        point x0 = .3*randpoint();
        analyze(a,f,fprime,x0,&period[k],&lyapunov[k]);
    }

    analyze(a,f,fprime,point(0,-1),&period[5],&lyapunov[5]);
    for(k=6;k<INITIALTESTS;k++)
    {
        point x0 = .5*randpoint();
        x0.y -= 1;
        analyze(a,f,fprime,x0,&period[k],&lyapunov[k]);
    }

    int sound=0;
    for(k=0;k<INITIALTESTS;k++)
        if(period[k] != -1)
        {
            lyapunov1[sound]=lyapunov[k];
            period1[sound]=period[k];
            sound++;
        }

/* the idea here
 * is to only consider non-divergent points when drawing lyapunov exponents
 * or periods. The initial point may have been just outside the basin of attraction
 * and we don't want to completely dismiss it. Similarly, if it is divergent,
 * then it will skew the period and lyapunov exponents for the points that *do* stay
 * inside the actual system.
 */
   if(sound>0)
   {
        double ratio = (double)sound/INITIALTESTS;

        double lyapunov0=0;
        for(k=0;k<sound;k++)
            lyapunov0 += lyapunov1[k];
        lyapunov0/=sound;

        int numberof[PERIODTEST];
        for(k=0;k<PERIODTEST;k++)
```

```
    numberof[k]=0;

for(k=0;k<sound;k++)
    numberof[period1[k]]++;

/*
// This was used to generate maps that featured
// systems with only one period.
int testnumber = 8;
if(numberof[testnumber]>0)
{
    float val = (float)numberof[testnumber]/INITIALTESTS;
    view[X][Y]=color(val,val,val);
}
continue;
*/

if(numberof[0]>0) // contains chaos, draw as lyapunov
    view[X][Y]=color((1-squash(lyapunov0)),0,squash(lyapunov0));

else if(numberof[period1[0]]==sound)
{
    // purely periodic (these are important areas)
    double r=(double)(period1[0]-1)/PERIODTEST;
    view[X][Y]=color((1-r),1,(1-r));
}

else
{
    // contains *multiply* convergent periods,
    // and *no* non-periodic cycles...
    // which is strange indeed.

    /*
    // This was in place to provide a special color for this situation
    // which would contain a fair bit of information, as it turned out
    // the extra information was just confusing

    int minp=PERIODTEST,maxp=0;
    for(k=0;k<sound;k++)
    {
        if(period1[k]<minp) minp = period1[k];
        if(period1[k]>maxp) maxp = period1[k];
    }

    double r1=(double)(minp-1)/PERIODTEST;
    double r2=(double)(maxp-1)/PERIODTEST;
    if(numberof[minp]+numberof[maxp] == sound)
        view[X][Y]=color(1-r1,1,1-r2);
    else
        view[X][Y]=color(1-r1,1-squash(lyapunov0),1-r2);
    */

    // this coloring produces dark green or brown colors
```

```
                view[X][Y]=color(1-squash(lyapunov0),squash(lyapunov0),0);
            }
        }
        else // divergent
            view[X][Y]=color(0,0,0);

    }}
    WriteBMP("out.bmp");

    return 0;
}
```

### A.4.4 henon julia.cpp

```
#include <stdlib.h>
#include <math.h>
#include <iostream>
#include <fstream>
#include <time.h>
#include <vector>

using namespace std;

#include "bitmap.h"
#include "base.h"
#include "dyn.h"


point f(parameter_set* a, point x)
{
    return point( a->a - x.x*x.x + a->b*x.y , x.x );
}

// DOTS is defined to produce an image that is black save for
// the points where an orbit converges to
//#define DOTS

int __cdecl main()
{
    srand((unsigned)time(0));

    int k,X,Y;

    double lyapunov;
    int period;

    // period is 0 if nonconvergent
    // -1 if goes to infinity
    // a positive integer if any other period

    double resolution = 10.0;
    double xcenter = 0.0;
```

```
    double ycenter = 0.0;

    parameter_set a(-1.4,-.3);

    for(X=0;X<RES;X++)
    {
    cout << X << endl;
    for(Y=0;Y<RES;Y++)
    {
#ifndef DOTS
        point x0 = point((resolution*X)/RES-.5*resolution+xcenter,
                -(resolution*Y)/RES+.5*resolution+ycenter);
        point x1 = x0;

        analyze(a,f,fprime,x0,&period,&lyapunov);

        if(period!=-1)
        {
            for(int i=0;i<5000;i++)
                x1 = f(&a, x1);

            view[X][Y] = color(.5+.5*squash(x1.x),
                .5+.5*squash(lyapunov), .5+.5*squash(x1.y));
        }
        else // divergent
#endif
            view[X][Y] = color(0,0,0);

    }}

#ifdef DOTS

    // sample random points until one is found which does not explode
    bool good = false;

    point x2;
    for(int tests=0;tests<1000 && !good;tests++)
    {
        cout << "testing: " << tests << endl;
        x2 = 1.5*randpoint();
        good = true;
        for(k=0;k<10000 && good;k++)
        {
            x2 = f(&a, x2);
            if(fabs(x2.x)>100 || fabs(x2.y)>100)
                good = false;

            if(k%100==0)
                cout << "x: " << x2.x << ", y: " << x2.y <<
                endl;
        }
    }

    // then draw its orbit
```

```
    // its color is given as a transition from red to blue
    // to help illustrate the folding nature of some orbits.

    if(good) for(k=0;k<10000;k++)
    {
        x2 = f(&a, x2);
        if(fabs(x2.x-xcenter)<resolution && fabs(x2.y-ycenter)<resolution)
        {
            float ratio = (float)k/10000;
            int ix =  RES*(x2.x/resolution + .5 - .5*xcenter);
            int iy = RES*(-x2.y/resolution + .5 + .5*ycenter);
            view[ix][iy] = color(1-ratio, 0, ratio);
        }
    }
#endif

    cout << "writing BMP\n";
    WriteBMP("out.bmp");

    return 0;
}
```

# B References

# References


[1] V. V. Nemytskii and V. V. Stepanov. *Qualitative Theory of Differential Equations*. Dover, New York, (1989)

[2] Lennart Carleson and Theodore W. Gamelin. *Complex Dynamics*. Springer-Verlag, New York, (1993)

[3] Einar Hille. *Ordinary Differential Equations in the Complex Domain*. Dover, New York, (1997)

[4] Edward Ott, Celso Grebogi, and James A. Yorke. *Controlling Chaos*. Phys. Rev. Lett. 64, (1990)

[5] G. A. Leonov. *Lyapunov Exponents and Problems of Linearization. From Stability to Chaos*. St. Petersburg University Press, St. Petersburg, (1997)

[6] Helena E. Nusse and James A. Yorke. *Characterizing the basins with the most entangled boundaries*. Ergod. Th. & Dynam. Sys. 23, (2003)

[7] Thomas J. Taylor. *On the existence of higher order Lyapunov exponents*. Nonlinearity. 6, (1993)

[8] Divakar Viswanath. *The fractal property of the Lorenz attractor*. Physica D. 190, (2004)

[9] Divakar Viswanath. *Symbolic dynamics and periodic orbits of the Lorenz attractor*. Nonlinearity. 16, (2003)

[10] Brian R. Hunt. *Maximum local Lyapunov dimension bounds the box dimension of chaotic attractors*. Nonlinearity. 9, (1996)

[11] J. J. Szczyrek. *Hausdorff dimension of a limit set for a family of nonholomorphic perturbations of the map* $z \to z^2$. Nonlinearity. 12, (1999)

[12] Marcy Barge and Sarah Holte. *Nearly one-dimensional Hénon attractors and inverse limits*. Nonlinearity. 8, (1995)

[13] Christoph Bandt and Karsten Keller. *Symbolic dynamics for angle-doubling on the circle: II. Symbolic description of the abstract Mandelbrot set*. Nonlinearity. 6, (1993)

[14] Karsten Keller. *Invariant factors, Julia equivalences, and the (abstract) Mandelbrot set*. Springer, New York. (2000)

[15] H. Bruin and M. Van Noort. *Nonconformal perturbations of* $z \to z^2 + c$*: The 1:3 resonance*. Prepublished, to appear in Nonlinearity.

[16] B. Krauskopf and H. Kriete. *Note on non-converging Julia sets*. Nonlinearity. 9, (1996)

[17] Bernd Krauskopf and Hartje Kriete. *Hausdorff Convergence of Julia Sets*. Nonlinearity. 9, (1996)

[18] Hartje Kriete. *Continuity of filled-in Julia sets and the closing lemma*. Bull. Belg. Math. Soc. 6, (1999)

[19] Marta Kosek. *Hölder continuity property of filled-in Julia sets in* $\mathbb{C}^n$. Proceedings of the American Mathematical Society. 125, (1997)

[20] Paul Bourke. *Random Attractors found using Lyapunov Exponents*. `http://astronomy.swin.edu.au/~pbourke/fractals/lyapunov/`

[21] J. C. Sprott. *Strange Attractors: Creating Patterns in Chaos*. M&T Books, New York. (1993)

[22] O. E. Rossler. *An equation for continuous chaos*. Phys. Lett. 35A, (1976)

[23] T. Y. Li and J. A. Yorke. *Period three implies chaos*. Amer. Math. Monthly 82, (1975)

[24] B. Bielefeld, S. Sutherland, F. Tangerman, J. Veerman. *Dynamics of certain non-conformal degree-two maps of the plane*. Experiment. Math. 2, (1993)

[25] David Ruelle. *Chaotic Evolution and Strange Attractors*. Academia Nazionale Dei Lincei, (1989)

[26] Ricardo Antonio Olivia. *On the Combinatorics of External Rays in the Dynamics of the Complex Henon Map*. PhD dissertation, Cornell University, (1998)

[27] Adrien Douady. *Does the Julia set Depend Continuously on the Polynomial* in R. L. Devaney (Ed.), Proceedings of Symposia in Applied Mathematics, 49, (1994)

[28] Romain Dujardin. *Hénon-Like Mappings in* $\mathbb{C}^2$. American Journal of Mathematics, 126, (2004)

[29] M. Hirsh, S. Smale. *Differential Equations, Dynamical Systems, and Linear Algebra*. Academic Press. (1974)

[30] Jack Hale. *Ordinary Differential Equations*. Wiley-Interscience. (1969)